Adult Stem Cells and Niche Cells segregate gradually from common precursors that build the adult Drosophila ovary during pupal development

Short title: Drosophila ovarian FSC and niche cell development

Amy Reilein[#*], Helen V. Kogan[#], Rachel Misner, Karen Sophia Park, Daniel Kalderon*

Department of Biological Sciences, Columbia University, New York, USA

[#] equal first authors

* corresponding authors: areilein@gmail.com, ddk1@columbia.edu

Summary

Adult stem cell function relies on the prior development of appropriate numbers and spatial organization of stem cells and supportive niche cells. Drosophila Follicle Stem Cells (FSCs) present a favorable paradigm for understanding those developmental processes. About sixteen FSCs in an adult germarium produce transit-amplifying Follicle Cells (FCs) from their posterior face and quiescent Escort Cells (ECs) to their anterior. Both ECs and FCs also act as niche cells. Here we show that adult ECs, FSCs and FCs derive from common precursors intermingled with germline cells during pupal development, with progeny of a single precursor commonly including ECs and FSCs, FSCs and FCs, or all three adult cell types. Precursors posterior to germline cells become the first FCs and engulf a largely naked germline cyst projected out of the germarium to form the first egg chamber and set up a key posterior signaling center for regulating adult FSC behavior.

Introduction

Adult stem cells generally act as a community, coordinating the activities of multiple individual cells to replenish tissues throughout life [1, 2]. The behavior of stem cells is invariably regulated by external signals from other cell types, known as niche cells [3-5]. It is therefore essential to establish adult stem cells in suitable numbers and niche environments during development to ensure appropriately regulated community activity in adults. Understanding the underlying developmental processes would facilitate identification of genetic developmental defects that confer deficiencies in adult tissue repair or cancer susceptibility, as well as the creation of functional organoids that are maintained by stem cells for therapeutic use, drug studies or mechanistic investigations [6-11].

The development of most terminally differentiated adult cell types results from a series of successive, definitive and largely irreversible decisions that are stabilized by potentially long-lasting shifts in gene expression and chromatin modification [12-17]. However, the development of adult stem cells has not been studied extensively and presents a number of special considerations. First, stem cells typically continue to proliferate in adulthood and often exhibit malleable relationships with their products, with the potential for marked changes in inter-conversion rates in either direction [18-20]. Does the general paradigm of definitive cell type specification at a fixed time in development still apply, despite this marked flexibility of the final product? Second, do adult tissues and the stem cells that maintain the tissue derive from separate or common precursors? Third, is there coordination between the development of adult stem cells and their niche cells, potentially serving to arrange appropriate proportions and juxtaposition of the two cell types?

Drosophila ovarian Follicle Stem Cells (FSCs) present a particularly interesting and experimentally favorable paradigm to investigate because the organization, behavior and regulation of these adult stem cells has been studied thoroughly, revealing many similarities to the important mammalian paradigm of gut stem cells [21-23]. FSCs also exhibit several interesting, potentially

53 prototypical features. FSCs directly produce two different types of cell in adult ovaries, Follicle Cells
54 (FCs) and Escort Cells (ECs) [23]. Both of these cell types also act as niche cells, producing key JAK-
55 STAT and Wnt signals, respectively [23-27]. Paneth cells in the mammalian small intestine are also
56 stem cell products and niche cells [28-30]. FSCs also provide a window into sustaining a tissue
57 supported by two different types of stem cell. The continued production of egg chambers involves
58 cooperation of somatic FSC products, ECs and FCs, with germline cells supplied by Germline Stem
59 Cells (GSCs) [22, 27, 31]. The mechanisms of coordination among FSCs, GSCs and their products in
60 the adult are currently not well understood but must rely on an organization that is established during
61 development [32].

62 GSCs and FSCs are housed in the germarium, which is the most anterior region of each of the
63 30-40 ovarioles comprising the adult ovary (Fig. 1J) [22]. Somatic Terminal Filament (TF) and Cap
64 Cells at the anterior of the germarium are stable sources of niche signals for GSCs and FSCs, including
65 BMPs (Bone Morphogenetic Proteins), Hedgehog and Wnt proteins, with GSCs directly contacting Cap
66 Cells [22, 31]. GSC Cystoblast daughters divide four times with incomplete cytokinesis to yield a
67 progression of 2-, 4-, 8- and finally,16-cell germline cysts. Their maturation is accompanied by posterior
68 movement and depends on interactions with neighboring quiescent, somatic ECs [33]. ECs also act as
69 niche cells for adjacent or nearby GSCs and FSCs [22, 27, 34, 35]. A rounded stage 2a sixteen-cell
70 cyst loses EC contacts as it forms a lens-shaped stage 2b cyst spanning the width of the germarium
71 and subsequently recruits FCs (Fig. 1J). The earliest FCs can be recognized by expression of high
72 levels of the surface adhesion protein, Fasciclin 3 (Fas3) [23, 36]. The stage 2b cyst rounds to a stage
73 3 cyst as surrounding FCs proliferate to form an epithelium and segregate specialized polar and stalk
74 cells, which allow budding of the FC-enveloped cyst as an egg chamber from the posterior of the
75 germarium (Fig. 1J) [37]. Polar Cells produce the JAK-STAT ligand, Unpaired, which patterns the
76 subsequent development of FCs along the AP axis of developing egg chambers [37-39] and creates a
77 gradient of signaling activity across the FSC domain, which is critical for FSC divisions and for FSC

conversion to FCs [24, 26]. Egg chambers bud roughly every 12h in each ovariole of well-fed flies, progressively enlarge and mature towards egg formation and deposition, as they move posteriorly.

There are about sixteen FSCs, which reside in three rings or layers around the inner germarial surface, between ECs and FCs on the AP axis (Fig. 1J) [22, 23]. The most posterior FSCs directly become FCs, while anterior FSCs directly become ECs, but FSCs also exchange AP locations, allowing a single FSC lineage to include both ECs and FCs [23]. Individual FSCs are frequently lost and frequently amplify, with no evident temporal or functional link between division and differentiation [40], so that the representation and output (of ECs and FCs) of any one FSC lineage is highly variable and stochastic [23]. All of these behaviors are largely regulated by extracellular signals that are graded along the AP axis, with especially prominent roles for JAK-STAT ligand derived from Polar Cells and Wnt ligands derived from both Cap Cells and ECs [23-25, 41, 42].

Previous studies have outlined how germline and somatic ovary precursors are first selected during embryogenesis, then migrate and coalesce to form a nascent gonad [43, 44]. The subsequent morphological organization of ovaries, constituent cell types and some information about relevant signals has been described up to the end of larval development [32, 45]. Understanding of pupal development is informed by a series of electron micrographs and a description of some key morphological processes [45-49] but has been limited, until recently, by technical difficulties associated with dissecting and imaging pupal ovaries [50]. Here we use morphological examination of developing pupal ovaries through fixed and live images, together with cell lineage studies to examine how adult FSCs, ECs and FCs are produced and organized from precursors present at the end of larval stages.

Marked cells derived from a single precursor clustered together along the AP axis but often spanned the border between adult EC and FSC territories. Thus, the key organizing principle guiding fate outcomes for ECs and FSCs appears simply to be a progression towards final cell locations along the AP axis without commitment to separate EC and FSC fates at a specific developmental time. The physical location and movement of precursors during the pupal period was clarified by morphological studies, including live imaging, showing that ECs and FSCs derive from precursors known as

Intermingled Cells (ICs), interspersed with germline cells in the developing germarium. A more posterior group of cells gave rise to the FCs of the first-formed egg chamber. Live imaging showed that the first pupal egg chamber is formed by migration of a germline cyst out of the developing germarium into an accumulation of future FCs, rather than emergence of an FC-encased germline from the germarium that characterizes adult egg chamber budding.

The major conclusions of common precursors for FSCs and their adult niche and product cells, ECs and FCs, together with an IC origin of FSCs both directly contradict recent conclusions made from limited, targeted lineage studies [51]. We repeated those targeted lineage approaches and found results consistent with the conclusions described above. Thus, the segregation of future stem cells from niche cells in this paradigm is a gradual process, rather than a rigidly imposed demarcation of different cell types delivered at a fixed time. The juxtaposition of adult ECs and FSCs, and derivation of appropriate numbers of ECs and FSCs is assured in part by their emergence from shared precursors and from an evolving AP gradient of proliferation.

119 # Results

120 ## Outline of ovary development

121 We dissected and imaged developing ovaries during pupation to provide a systematic
122 descriptive timeline (Fig. 1). Germaria within each ovary develop at slightly different rates (from medial
123 to lateral) and the overall duration of pupation can vary significantly, leading to some differences in the
124 reported timing of critical stages [46, 52, 53]. In common with other studies, we assign "0h APF (After
125 Puparium Formation)" as the time when larvae cease moving (pupariation) and used that event to
126 collect animals at known intervals after pupariation. Animals mostly eclosed up to five days later (120h
127 APF) and the first egg chamber had budded from about half of all germaria at about 56h APF (Fig. 1H).

128 Early ovary organization progresses from anterior (generally termed apical at early stages) to
129 posterior ("basal") (Fig. 1) [32, 45]. By the end of the third larval instar, each ovary has 15-20 anterior
130 stacks of non-dividing Terminal Filament (TF) cells (Fig. 1J), which characteristically express Lamin-C
131 but not Traffic Jam (TJ) (cyan arrowheads in Fig. 1D-F) [45, 54, 55]. "Apical cells" (white arrowheads,
132 Fig. 1A, G), initially anterior to the TF stacks migrate towards the posterior (basally), first separating
133 each TF stack and then entire developing ovarioles over the next 48h as they form an epithelial sheath
134 lined by a basement membrane [46]. The most posterior "basal cells" arise from swarm cells that
135 migrated from anterior locations prior to the late larval stage [56]. Fas3 expression initiates in a subset
136 of basal cells on the medial side of the ovary (pink arrowheads, Fig. 1B, C) [52], spreads across the
137 developing ovary and is then restricted to cells of epithelial appearance that intercalate progressively
138 from posterior to anterior, to form a basal stalk (pink arrowheads, Fig. 1E-G) at the posterior end of
139 each developing ovariole (Fig. 1J) [45, 57].

140 Developing germaria consist of germline cells (green in Fig. 1) and somatic cells (white in
141 Fig.1A-I) between the TFs and basal cells. About six of these somatic cells surround the most posterior
142 TF cell, the Transition Cell, and become non-dividing Cap Cells (Fig. 1J) [54]. Cap cells secrete
143 Perlecan, which is essential in forming the GSC niche [58]. Cap cells also express Lamin-C and TJ

144 shortly after the larval/pupal transition in response to Notch signaling and an ecdysone pulse [54, 59-
145 62]. Primordial germline cells (PGCs) that contact Cap Cells largely remain in position to become adult
146 Germline Stem Cells (GSCs) [63, 64]. The remaining PGCs develop similarly to adult Cystoblasts to
147 produce 2-, 4-, 8- and finally, 16-cell germarial cysts during pupation.

148 The somatic cells posterior to Cap Cells in the developing germarium are interspersed amongst
149 germline cells and were therefore named Intermingled Cells (ICs) (Fig. 1J). These cells express TJ
150 (white in Fig. 1A-I) but not Lamin C or Fas3 (both red in Fig. 1B-I) at pupariation, allowing for a clear
151 distinction from Cap Cells and basal cells [32, 52, 54]. It has generally been assumed that ICs are the
152 source of adult ECs [32] but neither this relationship nor the source of FSCs and FCs in newly-eclosed
153 adults has been clearly defined experimentally. Here, we use lineage analyses and the changing
154 morphology of developing ovarioles during pupation to investigate the origin of adult ovarian somatic
155 stem and niche cells.

156

157 **Spatially organized progression of germline differentiation**

158 We are principally interested in understanding the developmental origins of somatic ECs, FSCs
159 and FCs but this process must also be coordinated with germline development to produce egg
160 chambers, starting midway through pupation. Germline development was monitored by using Hts
161 antibody (red in Fig. 2) to reveal a rounded spectrosome, an internal organelle characteristic of single
162 germline cells, or a branched spectrosome derivative known as a fusome, which connects Vasa-
163 marked germline cells (green in Fig. 2) in a cyst [65], and by incubating samples with EdU to assess
164 DNA replication as a proxy for cell division (Fig. S1).

165 Primordial Germ Cells (PGCs) do not initiate differentiation before late larval stages due to the
166 repressive actions of ligand-free ecdysone receptor and Broad transcription factor targets in somatic
167 cells [60]. Thereafter, anterior PGCs receive BMP signals from newly-formed Cap cells that prevent
168 differentiation, allowing them to become adult GSCs, while posterior PGCs start to express the early
169 differentiation marker, Bam-GFP in late third instar larvae just prior to pupariation, co-incident with a

170 strong ecdysone pulse [60, 64]. A short time later, some branched fusomes are seen in posterior
171 PGCs, indicating divisions with incomplete cytokinesis to form cysts with 2 or more cells [53, 60]. The
172 subsequent progression of germline differentiation during pupation has not been described.
173 We observed 2-cell cysts at 0h APF, cysts of up to 8 cells by 12h APF, and 16-cell cysts at 18h
174 APF (Fig. 2A-C). Progressively larger cysts were arranged, with few exceptions, from anterior to
175 posterior from 18h APF onwards; this was particularly clear in samples from 24h to 48h APF (Fig. 2D-
176 F). Individual germaria within a developing ovary exhibited significantly different degrees of
177 progression, together with AP elongation of the germarium to accommodate increasingly large germ
178 cell units; in some cases, germline cells had also migrated posteriorly out of the germarial region, likely
179 as a non-productive developmental aberration (Fig. 2A-D). Two or more 16-cell cysts were seen in
180 individual germaria by 36h APF. A pair of posterior cysts were often side by side in germaria at 24h
181 APF but only a single cyst occupied the most posterior position in most cases by 36h APF, and in all
182 germaria by 48h APF (Fig. 2D-F). Consistent with these observations of cyst progression and location,
183 EdU labeling was often seen in the most posterior cyst(s) up to 24h but rarely at 36h, while at 48h even
184 the second most posterior cyst in the germarium rarely incorporated EdU (Fig. S1A-D). Our
185 observations reveal a progression of germline differentiation that is spatially organized along the AP
186 axis during the first 48h APF, at which time the organization of germline cysts resembles that in the
187 adult up to a stage 2b cyst (Fig. 1J).
188

189 **Follicle Stem Cells (FSCs) and Escort Cells (ECs) derive from a shared precursor**

190 We conducted a series of lineage analyses to learn about the specification of ECs, FSCs and
191 FCs from precursors during pupal development. In these studies, the timing of clone initiation was
192 deduced from the time elapsed between administration of a heat-shock to induce *hs-flp*-mediated
193 genetic recombination and adult eclosion. Thus, a "-5d sample" was generated by collecting very young
194 adults (less than a 6h range) centered around 120h after heat-shock (Fig. 3A). The time between
195 puparium formation and eclosion was generally a few hours more than observed for animals used in

196 morphological studies, but there is also a short delay between heat-shock and genetic marking of a cell
197 [66]. Consequently, the time a cell is genetically marked in a “-5d sample” likely corresponds closely to
198 puparium formation (0h APF) (Fig. 3A).

199 Ideally, a single precursor per developing ovariole would be labeled at a variety of times during
200 pupation, followed by comprehensive analysis of each resultant lineage in large numbers of ovarioles
201 from newly-eclosed adults. In practice, it is difficult to label only one cell in a developing ovariole when
202 there are many precursors present. We used a very mild heat-shock protocol to try to accomplish this
203 objective. We initially used MARCM clonal analysis [67] because positive cell marking with GFP greatly
204 facilitates scoring all cells in a clone. However, maturation of a strong GFP MARCM signal in adult and
205 developing ovarioles requires almost 4d. We therefore dissected ovarioles from adults 2d after eclosion
206 (“+2d”) in our first experiments, having induced clones daily (in separate experiments) between 6d and
207 2d before eclosion (“-6d” to “-2d”). These experiments provided an important overview of the temporal
208 progress of precursor types over the course of pupation (Fig. 3A). Subsequent experiments focused
209 further on studying single cell lineages by using multicolor labeling to reduce the frequency of labeling a
210 precursor in a specific color, and on capturing all labeled FCs produced during pupation by examining
211 lineages in newly-eclosed adults (Fig. 3A)

212 In the first experiments, involving staged clone induction, each ovariole in 2d-old adults was
213 scored for the number of marked FSCs (Fig. 1J), the number of marked ECs and the presence of
214 marked FCs in the germarium and first two egg chambers (implying the presence of a FSC 2d earlier)
215 by imaging and archiving complete confocal z-stacks (Fig. 3). Marked TF and Cap Cells were also
216 noted. Clones were classified according to inferred cell types present at the time of eclosion (see
217 Methods for extrapolating data from +2d adults to 0d adults).

218 The average number of labeled ECs and FSCs in a marked adult germarium decreased when
219 clones were induced at progressively later stages (from an average of 8.1 at -6d to 2.0 at -2d),
220 consistent with proliferation of most precursors during this period (Tables 1 and 2). Very few marked
221 clones were observed in the absence of heat-shock, consistent with almost all clones arising at the time

222 of deliberately administered heat-shock. As expected, TF cells were almost never labeled and Cap Cell
223 labeling was seen only at the earliest times of induction (present in 3% of clones induced at -5d (0h
224 APF)) because these non-dividing cell types have already differentiated shortly before (TFs) or just
225 after (CCs) the larval/pupal transition and the MARCM method only labels dividing cells.

226 Strikingly, almost all ovarioles with early-induced clones (from -6d to -4d) that included marked
227 FSCs also contained marked ECs ("EC/FSC clones") (Fig. 3A, D-G) (Table 1). Ovarioles containing
228 only marked ECs ("EC only") were seen at each time of clone induction, while a high frequency of
229 ovarioles with marked FSCs but no marked ECs ("FSC only") was evident only when induced at -3d or -
230 2d (Fig. 3A, K). These observations immediately suggested that most adult FSCs derive from a dividing
231 precursor that gives rise to both ECs and FSCs. During the second half of pupation an increasing
232 proportion of the products of early EC/FSC precursors produce FSCs but no ECs.

233

234 **Relative location of precursors along AP axis instructs fate**

235 We found that marked cells in an adult germarium were generally clustered in the AP
236 dimension. This can be seen for each time of clone induction by examining individual images (Fig. 3D-
237 K). To evaluate clustering numerically we counted marked region 1 (r1) and region 2a (r2a) ECs
238 separately. Region 1 contains germline cysts with fewer than 16 cells and comprises the most anterior
239 two-thirds of EC territory along the AP axis. Of all early-induced clones (-6d to -4d) with two or more
240 marked cells and including at least one r1 EC, 35% contained only r1 ECs, 19% included also only r2a
241 ECs, while only 8% also included only FSCs (the remainder included both r2a ECs and FSCs) (Fig.
242 3B). Thus, genetic relatives of a marked region 1 EC are often only in region 1; they are also more
243 commonly found in region 2a than in the more distant FSC region, even though the total frequency of
244 clones with marked region 2a ECs (54%) and FSCs (57%) were similar (Fig. 3B). Conversely, of all
245 clones with two or more marked cells including at least one FSC, 25% contained no ECs, 18% included
246 also only r2a ECs, while only 11% also included only r1 ECs, even though the total frequency of clones
247 with r1 ECs (68%) was higher than for r2a ECs (54%) (Fig. 3C). These observations support the

248 hypotheses that precursors occupy significantly different AP positions early in pupal development, their
249 progeny undergo stochastic movement in either direction but still remain relatively close in the AP
250 dimension, and cell identity (r1 EC, r2a EC or FSC) is set by their AP location at eclosion. By
251 adulthood, this identity includes starkly different behaviors of quiescence (ECs) or proliferation (FSCs).
252 Had precursors been restricted early in pupation to produce only FSCs, only ECs, or only one type of
253 EC (r1 or r2a), marked lineages would be restricted to a single cell type. In fact, we observed many
254 lineages that spanned boundaries between r1 and r2a ECs, and between ECs and FSCs, especially for
255 clones induced from 0h to 48h APF.
256

257 **Low frequency clones validate a common precursor for ECs and FSCs**

258 The overall clone frequency (percentage of ovarioles with any marked cells in the germarium or
259 early egg chambers) in the above experiments was 60%. It would therefore be expected that about 2/3
260 of marked ovarioles derive from marking a single precursor if all recombination events were
261 independent and equally likely (see Methods). To produce a higher frequency of ovarioles with marked
262 lineages derived from only a single cell we used a multicolor marking strategy. Here, recombination
263 events can lead to loss of GFP or a *lacZ* transgene, with or without RFP loss to yield six possible
264 lineage phenotypes, markedly reducing the proportion of precursors labeled by a specific color
265 combination (Fig3B) [23]. Two types of clone result from recombination at both *FRT40A* and *FRT42B*
266 (GFP-only and *lacZ*-only) and are therefore the least frequent. GFP-only clones, induced at -5d and
267 scored in newly-eclosed (0d) adults, were found at an overall frequency of 26/115 ovarioles, so that an
268 estimated 86% of labeled ovarioles (see Methods) would be expected to have lineages derived from a
269 single GFP-only cell.

270 The patterns of GFP-only and other multicolor clones were very similar to those observed by
271 MARCM analysis (Fig. 4), with a single lineage frequently spanning r1 and r2a territory, or EC and FSC
272 domains (Fig. 4A-C). Among GFP-only lineages that included FSCs, eight also included ECs and only
273 two did not (Fig. 4B, C). We can therefore be confident that a single precursor at -5d (0h APF) can give

274 rise to both ECs and FSCs and that most FSCs originate from such precursors. The proportions (and
275 yields) of GFP-only clone types were 42% EC-only (average 3.0 ECs), 31% EC/FSC (average 3.5 EC
276 and 2.6 FSCs) and 8% FSC-only (average 4.0 FSCs) (Table 3).
277 Clones of different colors in the same germarium were generally offset along the AP axis. In
278 some cases, the two differently colored clones likely derive from a single recombination event in a
279 common parent, yielding "twin-spot" daughters (Fig. 3B and Fig. 4D-F). These observations graphically
280 confirm the earlier conclusion that marked lineages spread a limited but significant distance along the
281 AP axis (even for the two daughters of a cell undergoing recombination), frequently spanning
282 boundaries between two different adult cell types.
283

284 **EC precursor division declines from the anterior at mid-pupation**

285 The MARCM lineage experiments, where lineages were induced at different times during
286 development, also yield information about when precursors of specific adult cell types stop dividing
287 because only dividing precursors can be labeled by mitotic recombination. For each time of clone
288 induction we summed the total number of marked cells of each type (FSCs, r1 and r2a ECs) over all
289 clones (Table 2). The ratio of marked ECs (r1 or r2a) to FSCs for any one time of clone induction
290 reports the relative number of those cell types produced from dividing precursors. The absolute number
291 of ECs made from dividing precursors was then calculated by using a value of 16 FSCs per germarium
292 and assuming that FSC precursors, like FSCs themselves, do not cease dividing (Table 2).
293 Importantly, this calculation is based on scoring all labeled cells over all clones and is therefore equally
294 valid whether the scored cells in an ovariole derive from a single marked cell or from more than one
295 marked cell.
296 For -6d and -5d samples, the calculated number of ECs made from dividing precursors was very
297 similar at about 33 (19 r1 and 14 r2a) per germarium (Table 2). This approximates the total number of
298 adult ECs, which has been reported to be about 40 on average [35], and which we counted as 32-51
299 over 25 germaria from young adults, suggesting that most cells that will become adult ECs are still

300 dividing at the larval/pupal transition. The calculated number of ECs made from dividing precursors
301 dropped slightly in -4d samples (from 33 to 28) and more markedly in -3d (to 15) and -2d samples (to
302 13) (Table 2). We surmise that precursors of over half of the future adult EC population have ceased
303 dividing by 2-3 days prior to eclosion. Moreover, the average number of dividing precursors for r1 ECs
304 (4.7) was significantly lower than for r2a ECs (8.6) by -2d (72h APF), even though adults contain more
305 r1 than r2a ECs (19 vs 14, from -6d and -5d data). Thus, a reduction in precursor division appears to
306 spread from the anterior towards the posterior as pupal development proceeds.
307 The inference of few, if any, non-dividing, and therefore potentially fully-differentiated, ECs
308 during the 0-24h APF period is notable because germline cells were found to develop from 1-2 cell
309 units into 16-cell cysts during the same period. These observations suggest that germline progression
310 can be supported by developing EC precursors.
311

312 **Some Follicle Cells produced during pupation derive from precursors that also yield**
313 **FSCs and ECs**

314 In a separate series of lineage experiments, we induced MARCM clones early enough (0h APF
315 and 36h APF) that we were able to examine GFP-labeled cells in newly-eclosed adults (Fig. 3A). This
316 allowed us to score all marked FCs produced from precursors, as well as FSCs and ECs, before the
317 earliest FCs are lost in 2d-old adults. From these data, we can learn about the developmental origin of
318 FCs, which are typically present surrounding the two most mature germarial cysts and four budded egg
319 chambers in a newly-eclosed adult (Fig3A).
320 We first examined lineages induced 5d before eclosion (at 0h APF). Most ovarioles with marked
321 FSCs also had marked ECs (24/27) (Fig. 5A, D), as observed in MARCM analysis in 2d-old adults and
322 multicolor clone analysis, confirming a common precursor of ECs and FSCs. Almost all clones with
323 marked FSCs also had marked FCs (25/27) (Fig. 5A), indicating a common precursor for adult FSCs
324 and FCs. A significant proportion of all marked ovarioles (23/98=23%) had marked ECs, FSCs and

325 FCs, indicating that some individual pupal precursors give rise to all three cell types in newly-eclosed
326 adults. Many ovarioles ("FC-only") contained marked FCs but no marked FSCs (Fig. 5C, D). Similar
327 results were observed for multicolor lineage tracing examined in newly-eclosed adults (Fig. 4, Table 3).
328 These results suggest that at the start of pupation there is a group of anterior precursors that produces
329 ECs, a group of posterior precursors that produces only FCs and a group of precursors in between that
330 produce a combination of two or three of these cell types (Fig. 6).

331 The locations of marked FCs were scored as "immediate" (region 2b), "germarial" (region 3) or
332 in egg chambers ("ECh") 1-4 (Fig. 3A and Fig. 7A). The percentage of clones with marked immediate
333 FCs was higher for ovarioles that included marked FSCs (56%) than for those without marked FSCs
334 (16%). Conversely, the percentage of ovarioles with marked FCs in at least one of the two terminal
335 (most posterior) egg chambers was higher when marked FSCs were absent (88%) than when they
336 were present (67%). Indeed, occupancy by marked FCs decreased gradually from anterior to posterior
337 for FSC/FC clones and with the opposite polarity for FC-only clones (Fig. 7A). Thus, derivatives of a
338 given precursor were clustered along the AP axis in FSC/FC territory, as previously noted for EC/FSC
339 territory. The inference that the fate of precursor derivatives is set largely by the AP position of
340 precursors, with limited AP dispersal of derivatives, appears to be the governing principle all the way
341 from the most anterior r1 EC derivatives to the most posterior FCs in newly-eclosed adults. Notably,
342 while some clones contained only ECs or only FCs, the AP spread of derivatives generally exceeded
343 the width of the FSC domain, so that ovarioles with marked FSCs always contained ECs or FCs (or
344 both). In other words, there were no FSC-specific precursors at the larval/pupal transition and individual
345 lineages regularly spanned the borders of adult cell identities (Fig. 6).

346

347 **Estimates of numbers of different precursors just prior to pupation**

348 The number of precursors at 0h APF that give rise to different adult cell types can be deduced
349 from the observed proportion of lineage categories (EC, EC/FSC+/-FC, FSC+/-FC, FC) together with
350 the average number of marked FSCs and ECs in each lineage category. However, both measured

351 parameters will be inaccurate if some ovarioles include two or more marked lineages. Analysis of
352 lineages in 0d adults allowed us to estimate how often this occurred.
353 In this MARCM experiment, 67% of 98 ovarioles contained no marked cells, suggesting that
354 80% of marked ovarioles have lineages derived from a single cell if all recombination events are
355 independent (see Methods). However, 16% of marked ovarioles contained marked FCs and marked
356 ECs but no marked FSCs, strongly suggesting that these discontinuous patterns represent two lineages
357 and hence, that the total proportion of ovarioles with more than one marked lineage is considerably
358 higher than 20%. Thus, there appears to be some clustering of recombination events rather than an
359 even distribution among all ovarioles, perhaps because temperature changes are not uniform during
360 the mild heat-shock conditions used to induce recombination events at a very low frequency. The
361 observed proportions of ovarioles with marked ECs and FCs roughly fit a simplified model where 30%
362 of ovarioles with any marked cells derive from a single marked cell and 70% derive from exactly two
363 marked cells (see Methods). We used that model to calculate the component single cell lineage
364 frequencies and component cell numbers per single-cell lineage that would give rise to the scored raw
365 data (see Methods). The deduced average number of dividing precursors at pupariation was about 24
366 in total, with 15.1 precursors giving rise only to ECs, 3.1 precursors producing ECs and FSCs, 1.2
367 precursors producing FSCs but no ECs, and 4.6 precursors producing only FCs on average (Fig. 5E;
368 Table 3).
369 Multicolor GFP-only clones were used previously to provide the most definitive evidence that an
370 individual precursor cell can produce both adult ECs and FSCs. The frequency of ovarioles with marked
371 ECs and FCs but no FSCs was only 8%, consistent with a high proportion of single cell lineages, which
372 we estimated at 70% (see Methods). From the inferred proportions of single lineage types and their
373 cellular contents (see Methods), we deduced that a single precursor cell gives rise to both ECs and
374 FSCs in 25% of all marked lineages and that the frequency of such precursors greatly exceeds
375 precursors that produce FSCs but no ECs (10%). The deduced proportions of clone types and the
376 number of precursors of each type (9.0 EC, 4.2 EC/FSC, 1.6 FSC, 2.4 FC and 17 total precursors) are

377 reasonably similar to those calculated above from the similarly timed MARCM experiment (Fig. 5E;
378 Table 3). Differences may result from variations in the exact developmental stage of animals of different
379 genotypes at the time of clone induction.
380 We also performed a MARCM analysis of clones induced 3.5d prior to eclosion (36h APF) and
381 examined in 0d adults to learn more about the timing of FC specification (see below). In this
382 experiment, the proportion of ovarioles that were labeled (94%) and the frequency of EC/FC clones was
383 particularly high, probably because there are many more dividing precursors than at 0h APF, so the
384 deduction of single cell lineage content is likely less reliable. Nevertheless, we estimated (see Methods)
385 that the proportions of single-cell lineage types were EC-only (51%), EC/FSC(+/-FC) (7%), FSC(+/-FC)
386 (4%), FC-only (38%) and that the total number of dividing precursors was about 35 (Fig. 5E; Table 3).
387 The most striking difference between lineages induced at 36h versus 0h APF is a large increase in
388 lineages producing only FCs. Based on earlier analysis of MARCM lineages induced at -4d and -3d and
389 examined at +2d, there should also be between 5 and 18 non-dividing EC precursors at -3.5d (Table 2).
390 Thus, we estimate that there are 13.3 FC-only precursors within a total precursor population of about
391 40-53 (35 dividing plus 5-18 non-dividing cells) at 36h APF (Table 3).
392

393 **Timing of FC recruitment to first egg chamber**

394 To determine when FCs are first allocated to the most mature germline cyst, we looked at the
395 distribution of marked cells in FC-only clones. The majority of newly-eclosed adults have four egg
396 chambers, and we excluded all exceptions from the analysis described below. For FC-only clones
397 induced at 36h APF, more than half (34 out of 49) included labeled FCs in the fourth (most mature) egg
398 chamber. Two-thirds of those (21 out of 34) had no other labeled FCs, showing that many precursors
399 are restricted by 36h APF to contribute only to the first-formed egg chamber (Fig. 7E, F). The 13
400 exceptions all had marked FCs in egg chamber 3 (Fig. 7E, G). This frequency is too high for all to be
401 explained by the presence of two lineages, and a single lineage might plausibly contribute to two
402 adjacent egg chambers. We also estimated the proportion of the egg chamber 4 epithelium occupied by

403 marked FCs. The proportion was significantly lower when marked FCs were also in egg chamber 3
404 (19.6%) than when confined to only the terminal egg chamber (29.7%) (Fig. 7B, D). These results
405 suggest that, in most cases, the initially labeled precursor at 36h APF divided before all egg chamber 4
406 FCs were allocated. In some cases, one daughter became an FC founder for egg chamber 4 and the
407 other daughter later contributed to egg chamber 3. In other cases, both daughters contributed to egg
408 chamber 4, accounting for a higher average FC contribution for that labeling pattern. We do not know
409 the cell cycle time for these FC-only precursors subsequent to 36h APF, but we expect (from
410 amplification data for EC/FSC lineages in Table 1) that it is shorter than 24h and may be as short as
411 11h, the cycling time for early FCs in adult ovarioles [68], so we estimate that FCs are allocated to egg
412 chamber 4 at about 47-60h APF. This estimate fits with later, direct morphological observations.
413 By 48h APF, all germaria have a single cyst in the most posterior region (Fig. 2) but neighboring
414 somatic cells (ICs) only express very low levels of Fas3 (Fig. 1G). In adult germaria, even the most
415 recently recruited FCs surrounding a stage 2b cyst express high levels of Fas3; a subset of those cells
416 must then become specialized polar and stalk cells before the egg chamber can bud a further 24h later
417 (Fig. 8J). The most posterior ICs that do not express Fas3 strongly before 48h APF therefore appear to
418 be far behind schedule, given that the first egg chamber will bud at about 56h APF on average (Fig. 1).
419 These observations raise the question of whether these ICs are indeed the cells that will form the FCs
420 of the first budded egg chamber, as might have been assumed by analogy to budding of adult egg
421 chambers.
422
423 **Lineage evidence for separate precursors of FCs in the first-formed egg chamber**
424 Marked FCs occupied only the two terminal egg chambers (one or both) in 35 out of 49
425 ovarioles with FC-only clones induced at 36h APF (Fig. 7E). Marked FCs occupied only territory
426 anterior to the two terminal egg chambers in five ovarioles, while the remaining nine ovarioles included
427 labeled FCs in terminal egg chambers and more anterior locations. It was estimated that most ovarioles
428 in this experiment have two marked lineages and that 38% of all single-cell lineages contain only FCs,

429 so around 11.5 of the 49 FC-only ovarioles (49 x $(0.38)^2$/[(2 x 0.38 x 0.62) + $(0.38)^2$]) might be expected
430 to include two FC-only lineages. Importantly, there were only two ovarioles with labeled FCs in egg
431 chamber 4 and also in locations anterior to egg chamber 3 (Fig. 6E) and these may plausibly contain
432 two lineages, consistent with a conclusion that, at 36h APF, precursors to FCs of the first-formed egg
433 chamber contribute only to egg chambers 3 and 4 (seen in 32/34 cases).

434 It is possible that the seven ovarioles with labeled FCs in egg chamber 3 (but not 4) and in more
435 anterior locations all harbor two lineages, but that seems unlikely since all seven have marked FCs in
436 egg chamber 2 (suggesting a common origin) and there were only 23 ovarioles with marked FCs in egg
437 chamber 3 altogether. Thus, by 36h APF the FC-only precursors appear to be segregated into two
438 populations. The majority contribute FCs to the first-formed egg chamber and sometimes also to egg
439 chamber 3, while the remainder contribute FCs to more anterior egg chambers, sometimes including
440 egg chamber 3. The AP location of different FC-only precursors at 36h APF presumably accounts for
441 these differences.

442 Ovarioles that included marked FSCs only rarely had marked FCs in the terminal egg chamber
443 (Fig. 6C). The five exceptions (out of 21) may derive from ovarioles that harbor an FC-only lineage
444 (53% frequency overall) in addition to an FSC-containing lineage (26% overall). Thus, at 36h APF it
445 appears that around two-thirds of FC-only precursors will contribute to the first-formed egg chamber,
446 with some of these also contributing to egg chamber 3, while more anterior egg chambers are later
447 populated by derivatives of a combination of FC-only, FSC/FC and EC/FSC/FC precursors.

448

449 **An Extra-Germarial Crown (EGC) forms prior to egg chamber budding**

450 Our cell lineage studies, in which any dividing cell can be labeled, provided information about
451 gradual restriction of precursor fates during pupation, according to cell locations along the AP axis. To
452 define the location of the precursors of FCs that coat the first budded egg chamber, we first examined
453 the changing morphology and gene expression patterns of developing ovaries. We already described
454 the onset of weak Fas3 expression in ICs as surprisingly close to the time of egg chamber budding

455 (Fig. 1), suggesting that ICs may not be the source of the first FCs because the first FCs most likely
456 already express Fas3 strongly.

457 Posterior to the interspersed germline cells and somatic ICs of the pupal germarium are somatic
458 cells with strong Fas3 staining from 24h APF onward (Fig. 1 and Fig. 8). We noticed that the most
459 anterior of these Fas3-positive cells express TJ, which is also expressed in ICs and required for their
460 interspersion with germline cells [69]. The TJ-positive cells form a small multi-layered cone or crown
461 around the posterior of the developing germarium that increases in size and cellular content from 12-
462 36h APF (Fig. 8A-C). We refer to those TJ/Fas3-positive cells beyond the most posterior germline cyst
463 as the Extra-Germarial Crown (EGC). A population of cells that expresses both TJ and Fas3 strongly is
464 notable because there is evidence from manipulation of TJ activity in adult ovaries that TJ generally
465 represses Fas3 expression [69], while a principal characteristic that distinguishes adult FCs from other
466 TJ-expressing cells (FSCs and ECs) is strong Fas3 expression (Fig. 8K) [23]. What becomes of the
467 newly-identified group of EGC cells, which express Fas3 strongly in addition to TJ?

468 In adults, a stage 3 germline cyst is separated from the most recently budded egg chamber by
469 only a small number of somatic cells (Fig. 1J and 8L). The stage 3 cyst then buds from the germarium
470 together with adjacent somatic FCs, which emerge as a monolayer epithelium connected to the
471 germarium by a thin, short stalk of specialized follicle cells. By contrast, prior to budding of the first
472 pupal egg chamber there is a large accumulation of somatic EGC cells posterior to the germarium (Fig.
473 8A-D) and after budding, the first egg chamber is often found much further from the germarium than in
474 adults (Fig. 1H). The intervening space is occupied by a partially intercalated stalk of TJ-negative cells
475 and by a small “secondary” EGC of Fas3- and TJ-positive cells, crowning the germarium (Fig. 8G).
476 After one cyst has budded and a second cyst has rounded up in preparation for budding (around 60h
477 APF) there is strong Fas3 expression in germarial somatic cells (Fig. 8J), resembling the pattern seen
478 in adults (Fig. 8K). In samples with two budded egg chambers (72-84h APF) or more, the newly budded
479 egg chamber is close to the germarium (Fig. 1I). Thus, formation of the first egg chamber appears to

480 involve a morphological process quite different from adult egg chamber budding; this is partly
481 recapitulated by the second egg chamber before adopting a typical adult morphology.
482

483 **Live imaging reveals EGC and basal stalk cells as the source of FCs for the first egg**
484 **chamber**

485 We used a live imaging protocol that we had previously developed for adult ovarioles [70] in
486 order to view pupal ovaries and track individual somatic cells. We were able to follow isolated live
487 ovaries for up to 15h, during which time many cell movements and cell divisions were observed,
488 suggestive of continued normal behavior. We first used samples where all cells were labeled by
489 expression of a *ubi-GFP* transgene. Later, we used animals with multicolor clones induced 2-3d earlier,
490 so that some cells had lost GFP or RFP expression or both (Fig 3B). Variability in the levels of GFP and
491 RFP simplified the task of following individual cells over time. We were able to track the movements of
492 multiple cells in a series of videos initiated at a variety of times after pupariation.

493 From about 30h APF onward, tracked ICs moved short distances relative to other cells in a
494 variety of directions. Most ICs maintained their relative AP locations within the developing germarium
495 as cysts moved past them. For example, one of two initially parallel germline cysts adopted the most
496 posterior position in the germarium while adjacent somatic ICs remained in position (Fig. 9A, B). Even
497 cells posterior to the most posterior cyst at 40h (red arrow, Fig. 9C), which are likely EGC cells (Fig.
498 8C), moved relative to the cyst to end up at the anterior of the cyst several hours later. At the same
499 time, an EGC cell (magenta arrow, Fig. 9C), initially distant from the cyst was adjacent to the cyst 9h
500 later. Another 40h APF movie similarly showed the cyst moving away from ICs (yellow, cyan, white,
501 magenta fill, in Fig. 9B) and making contact with EGC cells (outlined red cells, Fig. 9B). These
502 observations support the deductions from lineage analysis that precursors undergo limited, stochastic
503 movements along the AP axis and suggest that 16-cell germline cysts do not have a stable coating of
504 somatic cells from about 30-50h APF. Instead, by 48h APF the most posterior germline cyst is starting

505 to move into EGC territory. These observations are consistent with fixed images showing Fas3-positive
506 cells only posterior to the cyst at 36h APF (Fig. 8C-C") but beginning to surround the cyst by 48h APF
507 (Fig. 8D) because the cyst moves into the Fas3-positive EGC domain. During the 30-50h APF period,
508 there were cell divisions in the EGC and stalk (Movie S1) but we saw no evidence of cells moving from
509 the IC region into the EGC or in the reverse direction (see outlined red EGC cells in Fig. 9B),
510 suggesting that the EGC population grows primarily as a result of EGC cell division.

511 Imaging of an ovary from about 48h APF onwards captured the key process of egg chamber
512 budding for the first time (Fig. 10; Fig. S3-S5; Movie S2-S4). At 48h APF, fixed images showed that
513 cells surrounding the posterior half of the germline cyst express Fas3 strongly (Fig. 8D, yellow bracket),
514 consistent with evidence from live imaging that the cyst is already moving into EGC territory (Fig. 9B,
515 C), as described above. The location of Fas3-positive TJ-positive EGC cells is inferred (yellow and
516 green brackets, Fig. 10) by comparison to similarly-staged fixed images (Fig. 8), with Fas3-positive TJ-
517 negative cells posterior to the EGC considered basal stalk cells. The most posterior germline cyst
518 (highlighted by green nuclei in the lower germarium of Fig. 10) moved out of the germarium into EGC
519 territory, as EGC cells enveloped the cyst. For example, the cyan-outlined cell started within the EGC,
520 contacted the cyst prior to 8.3h and remained associated for the next 6.5h (Fig. 10; Fig. S4). Similarly,
521 the pink cell, initially just posterior to the cyst, moved to the midpoint of the budded egg chamber (Fig.
522 10; Fig. S3C; Movie S2). The red-outlined cell (red asterisk), which started on the posterior face of the
523 cyst, like the pink cell, initially maintained contact with the posterior-moving cyst. It was last seen at, or
524 just beyond, the anterior aspect of that cyst, suggesting it is moving past the cyst to contribute to the
525 secondary EGC, awaiting the second cyst to bud (Fig. 10; Movie S3).

526 IC cells were largely left behind in the germarium as the germline cyst moved into EGC territory.
527 The cells outlined in orange and green, like the yellow-outlined cell in the germarium above, started
528 close to the anterior face of the terminal cyst and lost contact with the cyst before 7h. At the end of the
529 imaging period, the cells outlined in orange and yellow were adjacent to the second cyst, inside the
530 germarium (Fig. 10; Fig. S3B and S5B). The green-outlined cell at 14:45h is in a location likely to

531 become the secondary EGC. The secondary EGC may therefore result from cells that were originally
532 ICs (green-outlined cell) and in the EGC (red asterisk).
533 Surprisingly, we observed that even distant basal stalk cells migrated onto the budding germline
534 cyst. The white-outlined cell, which initially lay posterior to the region with TJ expression (from
535 comparison to fixed images), entered EGC territory within 4h and became associated with the germline
536 cyst by 12h (Fig. 10; Fig. S4 and Movie S4). Thus, over the nearly 15h of live imaging the newly-
537 budded cyst acquired a set of closely-associated cells of epithelial appearance that derived from the
538 EGC and basal stalk cells, while tracked ICs at 48h APF were anterior to the budded cyst 15h later.
539 Live imaging of a different ovariole from 55h APF onward showed continued posterior
540 movement of the budding cyst until only a small number of basal stalk cells remained at its posterior
541 (Fig. 11B and Movie S5). During this almost 15h viewing period, the number of cells posterior to the
542 cyst declined from 32 to 13 (Fig. 11C). Fixed images of later stages, after two egg chambers have
543 budded (84h APF; Fig. 11D) revealed an average of 9 cells in the stalk posterior to the terminal egg
544 chamber, resembling the structure seen in newly-eclosed adults (Fig. 3A). Prior to budding, there were
545 50-65 cells posterior to the germline throughout the time range of 24 to 48h APF (Fig. 11A).
546 Thus, it appears that many cells in the basal stalk at 48h APF end up as FCs on the first budded
547 egg chamber, together with EGC derivatives. Some EGC cells likely pass over the entire budded cyst
548 to occupy the space between the germarium and the budded cyst, and may be joined there by some of
549 the cells that were the most posterior ICs at 48h APF to form the secondary EGC. It is very unlikely that
550 any ICs at 48h APF become FCs on the most mature egg chamber of newly-eclosed adults.
551 Imaging from about 60h APF onwards revealed the most posterior cyst in the germarium
552 rounding up and moving a short distance into the secondary EGC, which includes dividing cells (Fig.
553 S6A-C). Tracked cells on the first budded egg chamber moved short distances anterior as the stalk
554 elongated between the first and second egg chambers (Fig. S6C). ICs anterior to the second budding
555 cyst moved posterior as the germarium elongated and appeared poised to associate with later cysts
556 (Fig. S6A). We infer that the second budded egg chamber has FCs derived from the secondary EGC,

557 which is itself derived from primary EGC cells and, likely, some posterior ICs at 48h APF. FCs on later
558 egg chambers likely derive solely from cells that were ICs at 48h APF.
559
560 **Basal cell precursor contributions to the first-formed FCs and a basal stalk**
561 Live imaging indicated that many cells in the basal stalk at 48h APF later become FCs on the
562 first budded egg chamber, while a small number do not migrate over the cyst and form a short basal
563 stalk structure of 5-10 single-file cells posterior to egg chamber 4 in newly-eclosed adults (Fig. 3A).
564 Consistent with this scenario, when we examined lineages marked at 36h APF, we found 13 ovarioles
565 with label in the basal stalk and in FCs of egg chamber 4 (Fig. 7F, G), suggesting a common origin from
566 basal stalk cells at 36h APF. There were 18 ovarioles where FCs in egg chamber 4 were marked but
567 the adult basal stalk was not, consistent with an origin from EGC or anterior basal stalk cells at 36h
568 APF (Fig. 7E, H-J). The proportion of ovarioles containing marked FCs in egg chamber 4 that also
569 contained marked FCs in egg chamber 3 was higher when marked basal stalk cells were absent (7/18)
570 than when they were present (2/13), consistent with a more anterior origin of lineages that did not
571 include the adult basal stalk (Fig. 7E).
572 In summary, live imaging together with lineage analysis initiated at 36h APF revealed a
573 separate group of FC-only precursors, now identified as basal stalk and EGC cells posterior to the
574 germarium, that become FCs of the first-formed egg chamber and contribute also to the second-formed
575 egg chamber. Lineage analysis suggested there are additional FC-only precursors that contribute to
576 more anterior FCs. Those precursors may be located partly in anterior regions of the EGC at 36h APF
577 but it seems likely that most derive from ICs at 36h APF, given the observation that the germarium has
578 an adult morphology after two egg chambers have budded, with no EGC structure. Although we could
579 only track a subset of cells during live imaging, we did not find any evidence for cells posterior to ICs
580 entering the germarium at any stage, consistent with all ICs present in the germarium after two cycles
581 of budding originating from ICs at 36h APF. Importantly, the precursors of FSCs, which lie anterior to

582 FC-only precursors, must therefore arise from cells within the germarium (ICs) throughout pupal
583 development, whether they give rise to just FSCs and FCs or also to ECs.
584
585 **Pattern of precursor divisions along the AP axis**
586 The analysis of MARCM clones in 2d-old adults provided information about the pattern of
587 precursor divisions over time, based on the frequency of labeling specific precursors and the yield of
588 adult cells from each precursor (Table 1). There was a severe reduction in EC-only precursor division
589 rates from -4d to -2d (24h to 72h APF) with the frequency of such clones falling from 58% and 57% (-5d
590 and -4d) to 30% (-3d) and then 14% (-2d). Moreover, the decline in division spread from the anterior;
591 the yield of r1 ECs relative to r2a ECs declined from 2.2 (-5d) and 2.6 (-4d) to 0.9 (-3d) and 0.8 (-2d).
592 The yield of marked cells per EC/FSC or FSC precursor was consistently higher than for EC-only
593 precursors at all times of clone induction, indicating higher division rates in more posterior locations.
594 These yields underestimate EC/FSC and especially FSC precursor output because they do not include
595 FCs.
596 We also examined precursor cell cycling using EdU and FUCCI labeling. We incubated
597 dissected pupal ovaries at various developmental stages with EdU *in vitro* over a 1h time period to
598 detect cells in S phase. From 0-24h APF, ICs throughout the germarium often incorporated EdU (Fig.
599 S1A-C). By 48h APF, the prevalence of anterior EdU-labeled cells was quite low, whereas EGC cells
600 had frequent EdU signals (Fig. S1D). Even at 60h APF, however, an occasional IC in the anterior half
601 of the germarium could be found with EdU label; no anterior ICs labeled by EdU were evident at 96h
602 APF (Fig. S1E, F). At 96h APF some cells near the middle of the germarium but anterior to strong Fas3
603 expression, which may be r2a EC or EC/FSC precursors, did still incorporate EdU.
604 In the FLY-FUCCI system, RFP- and GFP-tagged proteins accumulate during the cell cycle
605 under the influence of a chosen promoter, while degrons from CycB and E2F1 promote rapid
606 degradation of RFP and GFP fusion proteins at the start of G1 and S phase, respectively [71]. While
607 RFP and GFP are expected to be reliably absent during G1 and S phase, respectively, the speed of

608 recovery of each signal during the next phase of the cell cycle depends on the strength of transcription
609 of FLY-FUCCI components. We used *UAS*-driven *FLY-FUCCI* transgenes and found *C587-GAL4* to be
610 more effective than *tj-GAL4* or *act-GAL4* in producing GFP and RFP FUCCI signals in the developing
611 somatic IC population and in adult ovaries. In adult germaria, all r1 ECs express only GFP (Fig. 12G),
612 indicating G1 (or a G0 state). r2a ECs include a mix of GFP-only G1 cells and cells with both GFP and
613 RFP, indicating G2 (Fig. 12G). FSCs additionally include some cells with RFP-only (late S-phase) and
614 no GFP or RFP (early S-phase, verified by co-labeling with EdU) (D. Melamed pers. comm.).
615 From 12-36h APF, ICs at all AP locations in the germarium included some cells with each
616 FUCCI color combination, although G1 cells were always most frequent in more anterior regions (Fig.
617 12A-D). By 48h APF, almost all somatic cells in the anterior half of the germarium were in G1 or G0
618 (GFP-only), consistent with substantially reduced cycling (Fig. 12E). A large fraction of EGC cells were
619 in S phase (marked by RFP only) (Fig. 12E'). By 96h APF, after two or three egg chambers have
620 budded, the *C587*-expressing domain had retracted anteriorly, roughly to territory anterior to strong
621 Fas3 staining and the pattern of FUCCI labeling was quite similar to adults, with anterior cells uniformly
622 in a G1 or G0 state, followed posteriorly by cells largely in G1 and G2 and then some cells in S phase
623 also (Fig. 12F). Thus, direct observation of EdU incorporation and cell cycle markers confirms the
624 progressive decline in anterior IC proliferation over time that was inferred from lineage analyses and
625 suggests that the anterior to posterior gradient of proliferation stretches all the way from the most
626 anterior ICs to posterior ICs and EGC cells, which appear to cycle rapidly.
627

628 **A putative FSC/FC precursor marker yields lineages that also produce ECs**

629 The location of precursors of a specific cell type can sometimes be deduced by taking
630 advantage of restricted gene expression patterns to target limited sets of precursors for lineage
631 marking. However, such approaches commonly suffer from limited targeting specificity and often do not
632 allow single-cell lineage tracing [72, 73]. If cell marking is not uniformly precise, it is challenging to link a
633 spectrum of initially marked cells with a spectrum of lineage outcomes because the same sample

634 cannot be examined at both the start and the end of an experiment to infer precursor-product
635 relationships directly. Recent single cell RNA sequencing of developing ovaries in late third instar
636 larvae led to the discovery of a variety of genes with regional expression patterns, providing resources
637 for targeted cell labeling [51]. The authors identified a cell population posterior to ICs that preferentially
638 expressed *bond* mRNA prior to pupariation. A *bond-GAL4* driver was then used together with a
639 temperature-sensitive *GAL80* transgene to initiate GFP-marked lineages using standard G-trace
640 reagents [74], keeping animals at 29C during larval stages to initiate labeling, switching to 18C (to
641 terminate labeling) about one day after pupariation and scoring marked cells in 2d-old adults [51]. Most
642 of the resulting labeled ovarioles (31/32) were described as including marked FSCs or FCs. FSCs were
643 not scored directly but were inferred from the presence of marked FCs in the germarium and youngest
644 egg chambers of 2d-old adults, and the fraction of 31 samples specifically with marked FSCs, rather
645 than just marked FCs, was not specified. More than half of the labeled ovarioles also contained marked
646 ECs (19/32). *bond-GAL4* expression was noted to be less specific than *bond* RNA, with some
647 expression in ICs in late 3rd instar larvae, while *bond* RNA was seen expressed throughout the IC
648 region in earlier 3rd instar larvae. Although the majority of ovarioles with marked FSCs evidently also
649 contained marked ECs, the authors suggested that separate precursors in these developing ovarioles
650 gave rise to ECs and to FSCs, with the latter situated posterior to ICs in late third instar larvae. Since
651 both of these conclusions are directly contradicted by our single-cell lineage analyses and
652 morphological studies, we investigated lineages targeted by *bond-GAL4* using reagents donated by the
653 authors. We scored results in newly-eclosed adults rather than 2d-old adults in order to count FSCs
654 directly, rather than inferring their presence indirectly, and to include also all FCs that are produced
655 from precursors during pupation.

656 We found a high frequency of GFP-marked cells when animals were kept at 18C throughout (37
657 labeled ovarioles out of 76), suggesting “leaky” clone initiation, with marked ECs or ECs together with
658 FSCs present in almost all cases (35/37) (Fig. 13A-D). We saw no increase in the proportion of
659 ovarioles with marked ECs or FSCs when larvae were raised at 29C before being moved to 18C about

660 2d after pupariation (eclosing 6d later; 13 of 44 ovarioles labeled), or when animals were raised at 18C
661 before shifting to 29C for the final 3d or 4d of pupation (23 of 88 ovarioles labeled) (Fig. 13D). Because
662 we observed no marked temperature dependence for these EC/FSC-containing clones we cannot
663 define the time at which cells were first marked. However, we expect that most lineages were initiated
664 close to the larval/pupal transition based on the composition of the lineages (see below) and because
665 TF and Cap cells were occasionally labeled.

666 The marked lineages were similar in their composition of cell types (Fig. 13A-D) to those we
667 described earlier using *hs-flp* to initiate clones at pupariation (5d before eclosion), suggesting that they
668 may have been induced at a similar time. The majority of ovarioles from the *bond-GAL4* experiments
669 (considering all three temperature conditions together) included either only marked ECs (about 40%) or
670 marked ECs and FSCs (about 50%, almost all together with marked FCs) (Fig. 11D). Only one out of
671 73 labeled ovarioles had marked FSCs (and FCs) but no marked ECs. These results clearly provide no
672 direct evidence of the labeling by *bond-GAL4* of precursors that produce FSCs and FCs without also
673 producing ECs.

674 The number of labeled ECs and FSCs (when present) per germarium was consistently higher
675 than we observed with *hs-flp* induced MARCM or multicolor clones induced at pupariation (Fig. 13A-C;
676 Table 3), suggesting that most labeled ovarioles in the *bond-GAL4* experiment contain lineages derived
677 from more than one precursor. The number of marked cells per ovariole was roughly consistent with the
678 output from two single-cell lineages in MARCM clones initiated at 0h APF. We therefore calculated the
679 component single clone types (frequency and number of products) that would produce the observed
680 *bond-GAL4 > G-trace* results if every ovariole had exactly two marked lineages (see Methods). The
681 inferred single precursor lineage types were similar to those induced by *hs-flp* at 0h APF (Fig. 11E;
682 Table 3). The most significant differences were a greater yield of ECs per EC-only lineage and fewer
683 FC-only lineages for lineages induced by *bond-GAL4*; both differences are consistent with slightly
684 earlier clone initiation. It is therefore likely that *bond-GAL4* labeled precursors sporadically throughout
685 the IC region, mostly shortly before pupariation. In keeping with our other lineage studies, inferred

686 single cell lineages that contained marked FSCs, also included marked ECs in almost all cases. The
687 source of lineages reported to include FSCs in the earlier study [51] may also have been pre-pupal ICs.
688 Moreover, the ovarioles with marked ECs and FSCs may have derived from common precursors,
689 consistent with all of our studies, rather than a combination of EC-specific and FSC-specific precursors,
690 as suggested by the authors [51].

691 When animals with *bond-GAL4* and *G-trace* were maintained at 29C during the last 3d or 4d of
692 pupation we observed an additional type of lineage, either in isolation or together with the types of
693 marked cells described above (55/88 ovarioles; 0/108 when at 18C throughout) (Fig. 13G). The second
694 lineage pattern consisted of a few isolated FCs or small FC clusters in the most mature egg chamber,
695 suggesting several independent recently initiated lineages. Some of the GFP-labeled FCs also
696 expressed *UAS-RFP*, indicating current or recent *bond-GAL4* activity (Fig. 13G). These patterns were
697 not reported previously [51] because the first-formed egg chambers are no longer present in 2d-old
698 adults. Surprisingly, the same type of clone was observed if animals were shifted from 29C to 18C
699 about 2d after pupariation (30/44 ovarioles, with only 6 ovarioles also including RFP-expressing FCs)
700 (Fig. 13F). The individual patches of marked FCs were much smaller than observed for lineages
701 induced by *hs-flp* at 36h APF and therefore presumably result from induction of multiple lineages at a
702 later time due to perduring *bond-GAL4* or *UAS-flp* products. The second pattern of lineages initiated by
703 *bond-GAL4* suggests selective expression of that marker in FCs of the first-formed egg chamber in late
704 pupae and adults. We have no clear evidence to evaluate whether *bond-GAL4* might also be expressed
705 sufficiently in precursors of those FCs to initiate lineages earlier in pupal development, reflecting the
706 posterior domain of *bond* RNA expression observed in late third instar larvae [51].
707
708
709

Discussion

An important general objective, exemplified here by FSCs, is to ascertain the origin of adult stem cells and surrounding niche cells in order to understand how their number and organization are instructed during development. Our investigations of changing morphology, cell movements and cell lineage reveal a gradual and flexible adoption of these cell types according to AP location throughout pupal development, rather than a series of discrete, definitive cell fate decisions (Fig. 6). This contrasts with the development of many other types of differentiated adult cells.

Specifically, adult EC niche cells and FSCs develop from a common group of dividing precursors (ICs) that are interspersed with developing germline cysts. ICs express TJ and are located posterior to Cap Cells, which serve as adult niche cells for both GSCs and FSCs, and are already specified by the start of pupation. The most anterior ICs become regional subsets of ECs (r1 and r2a), which likely have distinctive roles in the adult [75, 76]. These precursors markedly attenuate division, starting from the most anterior locations, during the second half of pupation (Table 2, Fig. 12 and Fig S1). ICs further from the anterior produce both ECs (mainly r2a) and FSCs, but EC production declines over time (Fig. 7). More posterior ICs produce FSCs and FCs (Fig. 6), while the most posterior ICs produce only FCs . The deduced pattern of germarium development ensures the juxtaposition of ECs and FSCs. The use of common precursors likely contributes to producing those cell types in appropriate proportions, while EC numbers are limited by a progressive decline in proliferation that spreads from the anterior.

Germarium development is likely driven in part by the early establishment of TF and Cap Cells as a source of organizing signals but the behavior of adult FSCs, including conversion to FCs, also relies on a signaling source posterior to the germarium [24, 26]. A key signal comes from specialized FCs, known as polar cells, on the most recently budded egg chamber (Fig. 1J). At the start of pupation there are no budded egg chambers, so formation of the first FCs and the first egg chamber must proceed by a different route. We found that those first FCs derive from precursors that are posterior to

735 ICs and differ from ICs during the first 48h of pupation by expressing Fas3 strongly, by lack of
736 association with germline cells and by being restricted to produce only FCs, and not ECs or FSCs.
737 Thus, the first population of posterior niche cells, and the most posterior portion of the ovariole of a
738 newly-eclosed adult are exceptional in being derived from precursors that do not overlap with the
739 precursors of adult FSCs.

740 Overall, almost the entire somatic cellular complement of the adult tissue that is subsequently
741 maintained by stem cell activity, derives from precursors that also produce adult FSCs. Preliminary
742 understanding of other adult stem cells suggests this arrangement may be common but not universal.
743 There is evidence that both adult mouse gut stem cells and adult neural stem cells of the dentate gyrus
744 derive from a common precursor pool that also gives rise to the adult epithelial tissue maintained by the
745 stem cell [77, 78]. By contrast, subventricular zone neural stem cells appear to be specified during
746 embryogenesis and remain quiescent, while the adult tissue it can replenish is built from other
747 precursors [79, 80].

748

749 **Defining and locating EC, FSC and FC precursors through pupal development**

750 This study is the first to examine Drosophila ovary development comprehensively during pupal
751 stages through lineage analyses initiated at different times, and by systematic analysis of fixed
752 specimens and live imaging. Each experimental approach included some challenges and leaves some
753 issues unresolved but several key findings appear conclusive and supported by all three approaches.

754 The challenge of labeling only a single precursor among many is common in lineage studies.
755 Here it was met by using very mild heat-shocks to initiate clones through *hs-flp* induction and a
756 multicolor labeling technique that reduces the frequency of a specific color combination substantially
757 relative to single-color clones. We were also able to evaluate the frequency of single-cell lineages from
758 both the overall frequency of ovariole labeling and the frequency of clone patterns (exceptional,
759 discontinuous clones), allowing us to derive mathematical estimations of strictly single-cell lineage
760 frequencies and yields. The results led to robust conclusions that many precursors at the start of

761 pupation yield only ECs, a smaller proportion yield both ECs and FSCs (as well as FCs) and very few
762 produce FSCs with no ECs. Common precursors for ECs and FSCs persist for at least the first 72h of
763 pupation (later times were not tested), although they are exceeded in number at 72h APF by precursors
764 that produce FSCs but not ECs. All such FSC lineages also included marked FCs in newly-eclosed
765 adults.

766 By 72-84h APF, after two egg chambers have been produced, the organization of the
767 germarium, including the pattern of Fas3 staining, appears similar to the adult germarium. It is therefore
768 plausible that the behavior of FSC precursors during the remainder of pupation is regulated just as in
769 adults, reflecting, in effect, completion of germarium development up to two days before eclosion. The
770 activity of common precursors for ECs and FSCs during the first half of pupation reflects a very different
771 process in a different environment, with progressive germline cyst differentiation being organized
772 simultaneously and no budded egg chambers to provide a key posterior signaling center. The
773 existence of common precursors for FSCs and ECs during the first half of pupation could not therefore
774 have simply been inferred or predicted on the basis of adult FSC behavior. Indeed, this finding, based
775 on painstaking lineage analyses, contradicts a previous conclusion [51]. The prior conclusion was
776 based on an approach that we also investigated, where marked lineages generally initiated from more
777 than one precursor in an ovariole, and generally also produced marked ECs when marked FSCs were
778 present. These results were previously interpreted as reflecting separate EC and FSC lineages in the
779 same ovariole in accord with a presumption of early fate specification based on differential gene
780 expression [51], but, in our hands, fit quantitatively with an origin from common EC/FSC precursors at
781 the start of pupation, in accord with all of our other lineage studies.

782 Our lineage studies provided some information about precursor locations. Each lineage was
783 restricted in its AP extent, but the whole collection of lineages included overlapping domains that
784 spanned the whole length of the ovariole of a newly-eclosed adult, from the most anterior r1 EC to FCs
785 and the basal stalk of the terminal egg chamber. Those observations strongly suggest that precursors
786 are arranged in a continuum along the AP axis throughout pupal development (Fig. 6). The anterior and

787 posterior limits of the EC/FSC/FC precursor domain were deduced from direct observation of pupal
788 development. Clone marking by heat-shock induction of Flp recombinase is through mitotic
789 recombination and can occur in any dividing cell. We directly observed EdU labeling in the most
790 anterior ICs in early pupae, so we can deduce that the most anterior of the inferred continuum of
791 precursors lie immediately adjacent to cap cells and give rise to adult r1 ECs. The posterior extent of
792 these precursors was deduced by direct observation, including live imaging, of the production of the
793 first FCs, as summarized below.
794

795 **Live imaging reveals the posterior origin, outside the developing germarium, of the first**
796 **FCs**

797 The precursors that give rise to FCs surrounding the most posterior egg chamber of newly-
798 eclosed adults were identified by a combination of fixed and live images. These cells all express Fas3
799 strongly by 24h APF and comprise two distinguishable groups according to their locations and TJ
800 expression prior to egg chamber budding. We named one group as Extra-Germarial Crown (EGC) cells
801 in recognition of their location and appearance. EGC cells accumulate from a handful to over twenty
802 during the first 48h APF. The second group of cells are further posterior, do not express TJ and are
803 largely intercalated into a stalk of 1-2 cell's width at 48h APF prior to egg chamber budding. During
804 budding, the most mature germline cyst leaves the germarium largely devoid of accompanying ICs,
805 which do not yet express Fas3 strongly. The cyst then enters EGC territory and moves a considerable
806 distance from the germarium as it is enveloped by EGC and basal stalk cells.

807 Towards the end of the budding process, cells posterior to the new egg chamber are stacked in
808 single file, forming a basal stalk, which is stably retained into adulthood, confirming and supplementing
809 prior descriptions of basal stalk formation [45]. We observed several lineages that included labeled cells
810 in the adult basal stalk and in a FC patch on the terminal egg chamber, reflecting contributions of pupal
811 basal stalk cells. Meanwhile, some EGC derivatives also remain on the first budded egg chamber, while

812 others migrate beyond the budded cyst to form a secondary EGC between the germarium and the
813 budded egg chamber. Secondary EGCs provide cells to partially coat the second cyst to emerge from
814 the germarium. The second cyst appears from live imaging to move out of the germarium together with
815 some associated ICs. Lineage studies also suggest that FCs of the second budded egg chamber derive
816 from both EGC cells (producing FCs in egg chamber 4 and 3) and ICs (producing FCs in egg chamber
817 3 and more anterior locations) (Fig. 7E). The budding of the third, and subsequent, egg chambers is
818 likely similar to the process in adults, with cysts emerging from the germarium completely encased by
819 FCs, as there is no longer a recognizable EGC after two egg chambers have budded and the two most
820 mature germline cysts are associated with strongly Fas3-positive cells within the germarium after the
821 second egg chamber is about to bud.
822 These observations and deductions not only reveal the posterior limit of EC, FSC and FC
823 precursors as including basal stalk cells at about 48h APF, but also provide evidence that FSCs derive
824 from precursors that are ICs. The evidence is temporal and numerical. First, we saw an expansion of
825 the EGC population from 12-48h APF prior to egg chamber budding (Fig. 8). During that time and
826 during the budding process, we did not observe any cells from the EGC moving into the germarium.
827 Moreover, as soon as the second egg chamber is about to bud, it is highly likely that the FCs of both of
828 the next two future egg chambers are the Fas3-positive IC cells that surround those cells in the
829 germarium. Those prospective FCs therefore almost certainly derive from precursors that were never
830 outside the germarium. FSCs derive from precursors that are further anterior, so those precursors were
831 even more certainly always within the germarium as ICs. Second, just as the first germline cyst leaves
832 the germarium at, or shortly after 48h APF, there are over 60 TJ-positive somatic ICs in the germarium
833 (Fig. 8D). At this time, many EC/FSC precursors are still dividing and not all future ECs have terminated
834 divisions. The total number of ECs (about 40 on average) plus FSCs (about 16) in an adult germarium
835 is less than 60, so it is clear that the ICs in the germarium at this time must include all EC and FSC
836 precursors and a significant number of FC precursors.
837

838 **Deductions from targeted lineage analyses**

839 A recent study used single cell RNA sequencing to explore the diversity of precursors in late
840 larval ovaries. Of most relevance here, it was suggested that a distinct group of cells posterior to ICs
841 and characterized by *bond* expression give rise to FSCs and FCs but not ECs [51]. As described
842 earlier, the supporting lineage studies and our reproduction of lineages initiated from cells expressing
843 *bond-GAL4* cannot be interpreted definitively because ovarioles almost never contained lineages
844 derived from a single cell. The results are nevertheless compatible with all of our other observations
845 demonstrating that FSC precursors at the start of pupation also give rise to ECs, and that FSC
846 precursors are ICs, residing within the developing germarium throughout pupation. Indeed, because we
847 scored FSCs directly, counted the number of labeled ECs and FSCs in each sample, and could
848 compare the results to those we had already obtained for single-cell lineages initiated at pupariation,
849 we were able to deduce that ovarioles almost always harbored more than one lineage initiated by *bond-*
850 *GAL4*. This allowed us to estimate the composition of single-cell lineages and found they were very
851 similar to those induced by heat-shock induction of marking in all dividing cells. Although temperature
852 control of initiation of clones with *bond-GAL4* was leaky, we can infer that the FSC-yielding lineages
853 mostly reflect initiation by *bond-GAL4* expression in ICs shortly before pupariation. This is compatible
854 with the observation that *bond-GAL4* is expressed at low levels throughout the IC region in mid-third
855 instar larvae [51].

856 We also observed another type of lineage when *bond-GAL4* activity was increased by raising
857 the temperature during pupal development. Here, labeled FCs were seen in small patches on the first
858 budded egg chamber. Those lineages would not have been apparent in the earlier study because only
859 2d-old adults were examined [51]. The labeled FC patches were much smaller than those induced by
860 lineages initiated at 36h APF, so they must reflect *bond-GAL4* expression in those FC precursors late in
861 pupation. We did observe sporadic *bond-GAL4* expression in FCs of the most mature egg chamber in
862 adults. It seems plausible that the expression of *bond* RNA observed posterior to ICs in late larvae [51]
863 may continue in an analogous location, posterior to the germarium, in the EGC or basal stalk, and as

those cells become FCs. However, at present, we have no direct evidence of *bond* expression during pupation or of lineages initiated in cells posterior to ICs prior to budding of the first egg chamber.

Coordination between germline and somatic ovarian cell development

Ovary development not only organizes suitable numbers of FSCs, GSCs and their niche cells into an adult germarium, ready to fuel lifelong adult oogenesis, but also initiates oogenesis very early, so that the first eggs can be laid shortly after eclosion. How is the posterior progression of increasingly mature cysts, starting from single anterior cells, organized?

Ecdysone acts positively in somatic cells of late third instar larvae to initiate GSC differentiation, manifest by induction of the differentiation factor, Bag-of-marbles (Bam) and then cystocyte formation, revealed by the transition of the rounded spectrosome to a branched fusome [59, 60]. Prior studies did not reveal whether Bam-GFP expression or PGC division initiates simultaneously in all PGCs distant from Cap Cells or in an anterior-posterior gradient, or how germline differentiation proceeds thereafter. We found that there is a clear anterior to posterior polarity of increasingly developed cysts that produced a mature steady-state pattern by 48h APF. This was deduced by counting the number of germline cells linked by fusomes, with 16-cell cysts first appearing 18h APF, and by observing the exclusion of EdU DNA replication signals from the most posterior regions of the germarium from 36h onwards, indicating occupancy by only 16-cell cysts. Moreover, a single posterior sixteen-cell cyst emerged for the first time between 36h and 48h APF.

These observations raise the question of what underlies the spatially organized initiation or progression of differentiation of PGCs that are in different locations at the larval/pupal transition. The BMP signals that maintain anterior pre-GSCs are likely highly spatially restricted, as in adults [81], while hormonal Ecdysone signals may be spatially uniform, suggesting that there must be other important differentiation signals. Potential sources of relevant signals are the adjacent somatic cell precursors, which will later become ECs. There is some evidence that the ordered posterior movement of germline cysts in adult germaria depends on EC interactions [82]. During pupal development, the situation is

890 different because the initiation of germline differentiation must be spatially organized and many EC
891 precursors are still dividing during this time. It will be interesting to investigate whether pupal EC
892 precursors or adult ECs have spatially graded adhesive properties or send graded differentiation
893 signals according to their AP position.
894

895 **Organizing patterned development of adult stem cells and niche cells**

896 It is common to think of developmental processes and cell types in terms of establishment of
897 transcriptional networks and key markers that bear witness to permanent decisions. Investigations of
898 adult FSCs, and other adult stem cell paradigms such as the mammalian gut, as well as the
899 observations described here regarding FSC development, reveal a more flexible process, in which
900 environmental signals reflecting current cell locations may be more significant than stable expression of
901 master regulators of transcription. For example, the transcription factor TJ is selectively expressed in
902 many developing and mature ovarian somatic cells, and it has been shown to be important for the
903 specification of Cap Cells and many IC derivatives [52, 54]. We therefore suspected that EGC cells,
904 posterior to ICs, might be FC precursors because they also expressed TJ. Although that suspicion was
905 supported by live imaging studies, the same studies showed that TJ-negative basal stalk cells also
906 became FCs. Thus, TJ neither defines ICs nor EC/FSC/FC precursors. We think it is likely that
907 studying the spatial distribution of external signals and their interpretation by somatic cells in the
908 developing ovariole will be essential to understand why some cells initially mix with germline cells to
909 become ICs, while others do not, and how these cells become ECs, FSCs and FCs just in time to serve
910 the appropriate functional role.

911 The signals that guide formation of Fas3-positive FCs in the adult germarium include low Wnt
912 pathway activity and high JAK-STAT pathway activity. The location of FC differentiation is set, at least
913 in part, by a Wnt pathway activity gradient that declines from the anterior and by the opposite polarity of
914 graded JAK-STAT pathway activity initiated by a ligand derived from polar cells of the previously
915 budded egg chamber [24, 26]. Prior to budding of any egg chambers in pupal ovaries, there is no polar

FC source of JAK-STAT pathway ligand. It will be interesting to discover whether differentiation of the first FCs in pupal ovaries also relies upon being distant from an anterior source of Wnt and perhaps other pathway ligands, such as Hedgehog, and whether a JAK-STAT signal, coming from a source other than polar cells, is employed.

Acknowledgments

This work was supported by NIH RO1 GM079351 to DK. We thank Ruth Lehmann, Dorothea Godt, Erika Bach, Ramanuj DasGupta and Ward Odenwald for reagents, Pegah Kohosravi-Kamrani, Shay Mallick, Aaron Choi and Jack Misner for help with experiments and analysis, David Melamed for continued discussions and input, the Bloomington stock center for provision of genetic reagents, the Developmental Studies Hybridoma Bank (DSHB) for antibodies, FlyBase as an information resource, and the confocal microscope resource provided by the Dept. of Biological Sciences, Columbia University.

Conceptualization, A.R. and D.K., Formal Analysis, D.K., Funding Acquisition, D.K., Investigation, A.R., H.K., R.M. K.P., Methodology, H.K., K.P., A.R., R.M. D.K., Supervision, A.R. and D.K., Validation, A.R., H.K., R.M., K.P., D.K., Visualization, A.R., H.K., R.M., Writing-Original Draft, D.K., Writing-Review & Editing, A.R., H.K., R.M., K.P., D.K.

934 # Materials and Methods

935 ## Staging of pupae

936 Third-instar larvae were sorted to select females, transferred to a vial with food and checked every hour
937 to mark the time each individual developed into a puparium (white, but immobile, with small anterior
938 spiracles). This time is 0 hours APF (after puparium formation). We found that keeping animals in the
939 light at night and in the dark during the day on a 12h/12h cycle, allowed more of them to pupate during
940 the daytime. We used a programmable outlet timer (Nearpow) together with a manual LED soft white
941 nightlight (Energizer cat. 37099) installed in a dark incubator at 25C.

942

943 ## Dissection and staining of pupal ovaries.

944 Pupae were removed from the vial wall by adding a drop of water and transferred with forceps into a
945 well of a Corning PYREX glass spot plate (Corning, cat. no. 7220–85) containing either PBS or 4%
946 paraformaldehyde solution with care taken not to damage or pierce the posterior end of the pupa. If the
947 dissection was done in fixative solution, it could take no longer than 10 min (ovaries were rocked in
948 clean fixative for a minimum of 15 min, but for no longer than 30 min). Ovaries from 72h APF and older
949 had fewer tears in them when dissected directly into fixative. Using a dissecting microscope, pupae
950 were held against the bottom of the well using forceps and the posterior tip was cut off using Vannas
951 Spring Scissors (2.5mm straight edge, Fine Science Tools, Foster City, CA, item number 15000-08)
952 about a third of the way in from the posterior end. The anterior part of the pupa was removed to a
953 discard well. The posterior end was searched for ovaries (clear, spherical, striated structures) by gently
954 dislodging fat tissue surrounding the ovaries so as not to cloud the well with debris. This was done by
955 gently tearing apart the contents of the pupal case or swirling them in the well using two pairs of
956 forceps. As soon as they were spotted, ovaries were transferred to a new well of fixative by the
957 following process. A 20µl pipette tip with a pipettor set to 20µl was coated in 10% Normal Goat Serum
958 (NGS) by pipetting up and down several times. The pipettor was set to 5µl to pipette up the ovary from

959 the dissection well to transfer into the fixative well. Ovaries were fixed by rocking in the well for 15 min
960 at room temperature. Fixative was removed with a 1000µl pipette set to 270µl to slowly and carefully
961 pipette up the liquid. The 1000 µl pipettor was used to remove liquid after all subsequent steps. Ovaries
962 were rinsed 3x in 2% PBST 0.5% Tween solution for 5, 10, and 45 min at 4C by rocking very slowly in a
963 horizontal plane. The glass dissection dish was covered with a large pipette tip box. Ovaries were
964 rinsed for 30-60 min in 10% NGS solution at 4C, and then rocked gently in primary antibody
965 overnight. Ovaries were rinsed 3x with 0.5% PBST and then incubated for 1 hour (covered, cold room,
966 rocker set on 2) in secondary antibody diluted 1:1000 with 0.5% Triton. Ovaries were rinsed 2x with
967 0.5% PBST and 1x with PBS. To mount ovaries, a 20µl pipette tip coated in 10% NGS solution as
968 described above was set to 5µl and used to capture the ovary and transfer to a glass slide. 20µl of
969 DAPI Fluoromount was added to a coverslip, and then placed on top of the slide with the ovaries. Care
970 was taken to avoid pressing the coverslip and potentially disfiguring the mounted ovaries. For older
971 pupal ovaries, specifically 72h APF and onwards, forceps were used to gently tear apart the ovarioles
972 to separate germaria for clearer imaging. A sharpie was used to draw arrows to mark the location of the
973 ovaries on the coverslip.
974

975 **EdU labeling**

976 Ovaries were dissected directly into 15µM EdU in Schneider's insect medium, incubated for 1h at room
977 temperature and then fixed for 10 min at room temperature in 4% paraformaldehyde. EdU incorporation
978 was detected using the Click-iT Plus EdU Imaging Kit C10637 (Life Technologies).

979

980 **Immunohistochemistry**

981 Monoclonal antibodies against LaminC, Fasciclin III, Vasa and Hts were obtained from the
982 Developmental Studies Hybridoma Bank, created by the NICHD of the NIH and maintained at The

983 University of Iowa, Department of Biology, Iowa City, Iowa 52242. 7G10 anti-Fasciclin III was deposited
984 to the DSHB by C. Goodman, and was used at 1:300 for multicolor lineage experiments and at 1:250 in
985 all other stainings. 1B1 anti-Hts was deposited by H.D. Lipshitz. LC28.26 Anti-LaminC at 1:50 was
986 deposited by P.A. Fisher. Anti-Vasa (used at 1:10) was deposited by A. C. Spradling/D. Williams and
987 used for staining adult ovaries. For pupal ovaries, the monoclonal rat anti-Vasa was not effective and
988 instead rabbit anti-Vasa (gift from R. Lehmann, NYU medical school) was used. Other primary
989 antibodies used were rabbit anti-Zfh-1 at 1:5000 (a gift from R. Lehmann, NYU medical school), guinea
990 pig anti-Traffic Jam at 1:5000 (a gift from Dorothea Godt, University of Toronto, Canada), anti-β-
991 galactosidase (Catalogue No. 55976, MP Biomedicals) at 1:1,000; anti-GFP (A6455, Molecular Probes)
992 at 1:1,000; goat FITC-anti-GFP (Abcam ab6662) at 1:400. Secondary antibodies were Alexa-488,
993 Alexa-546, Alexa-594 or Alexa-647 from Molecular Probes. Ovarioles from multicolor experiments were
994 mounted in Prolong Gold Antifade (Invitrogen). DAPI-Fluoromount-G (Southern Biotech) was used as
995 mounting medium for all other experiments. Images were collected with a Zeiss LSM700 or
996 LSM800 laser scanning confocal microscope (Zeiss) using a 63x 1.4 N.A. lens.
997

998 **Adult ovary fixation and staining**

999 Ovaries were fixed in 4% paraformaldehyde in PBS for 10 min at room temperature, rinsed three times
1000 in PBS with 0.1% Triton and 0.05% Tween-20 (PBST), and blocked in 10% normal goat serum
1001 (Jackson ImmunoResearch Laboratories) in PBST. Ovarioles were incubated in primary antibody for 45
1002 min for multicolor lineage experiments and overnight for all other experiments. Ovarioles were rinsed in
1003 PBST three times and incubated for 1 h in secondary antibodies diluted 1:1000.
1004

1005 **Live imaging and analysis**

1006 Live imaging was performed as in [70], except that pupal ovaries dissected in imaging medium were left
1007 intact instead of separating into individual ovarioles. Intact pupal ovaries were mixed with Matrigel in a

1008 well of a gas-permeable imaging chamber. Ovaries were of genotype *yw hs-flp; ubi-GFP FRT40A* (Ubi-
1009 GFP ovaries) or *yw hs-flp/yw; ubi-GFP FRT40A FRT42B His2Av-RFP/tub-lacZ FRT40A FRT42B*
1010 (referred to as multicolor ovaries). Clones were generated in the multicolor ovaries by two 10 min heat
1011 shocks at 37C spaced 8 hours apart, 48 to 72 hours before imaging in order to generate GFP-only and
1012 RFP-only cells that were easier to track. Images were acquired every 15 min with 2.5 µm between Z-
1013 stacks. Volocity Software (Quorum Technologies, Puslinch, Ontario, Canada) was used to make the 4D
1014 reconstruction of the UbiGFP labeled ovary. All nineteen z slices covering 45 µm were used in the
1015 reconstruction; however, germaria drifted during imaging such that FCs covering approximately one
1016 quarter of the budded egg chamber on the lower germarium were not imaged. Cells were colored with
1017 Procreate software (Savage Interactive, North Hobart, Australia). Germline cells in the UbiGFP movie
1018 were identified based on their larger size and paler labeling with GFP compared to somatic cells.
1019

1020 **Clonal analysis and FUCCI labeling genotypes**

1021 MARCM clones for lineage analysis were generated on 2R and 3R using the following
1022 genotypes: (2R) yw *hs-Flp, UAS-nGFP, tub-GAL4/ yw; FRT42D act-GAL80 tub-GAL80 /*
1023 *FRT42D sha; act>CD2>GAL4/* + and (3R) yw *hs-Flp, UAS-nGFP, tub-GAL4/ yw;*
1024 *act>CD2>GAL4 UAS-GFP / +; FRT82B tub-GAL80/FRT82B NM*
1025 For multicolor clones flies were of the genotype: *yw hs-flp/yw; ubi-GFP FRT40A FRT42B His2Av-*
1026 *RFP/tub-lacZ FRT40A FRT42B*
1027 Genotypes for FLY-FUCCI were *C587-GAL4/ yw; UAS-FUCCI/Cyo; UAS-FUCCI/ (UAS-FUCCI or*
1028 *TM6B)*.
1029

1030 **Lineage analysis by MARCM**

1031 Pupae were heat shocked at 33C for 12 min at the number of days indicated before eclosion. Flies
1032 were dissected on the day of eclosion (0d MARCM) or collected on the day of eclosion and dissected 2
1033 days later. Ovaries were stained using antibodies to Vasa, Fas3 and GFP. Cells were scored as r1 or
1034 r2a based on measurements that were performed to determine the lengths of these regions. To
1035 determine the boundaries of each region we examined EdU incorporation in ovaries of newly eclosed
1036 flies and measured the distance from cap cells to the end of Region 1 as determined by the presence of
1037 cysts that incorporated EdU. Region 1 cysts are going through mitosis and Region 2a cysts have the
1038 complete complement of 16 germ cells. The length ratio of Region 1:2a is about 3:1 in newly-eclosed
1039 adults. To measure the percentage of each egg chamber covered by marked FCs, GFP was used to
1040 count the number of marked FCs and DAPI was used to count the total number of FCs in each z
1041 section.
1042

1043 **bondGal4/G trace experiments**

1044 *bond-GAL4/G-TRACE* flies (a gift of Ruth Lehmann, NYU medical center) were crossed at 18C and
1045 either kept at 18C, shifted after egg-laying to 29C and shifted back to 18C in mid-pupation (flies took 6
1046 more days to eclose at 18C); or shifted to 29C 3 to 4 days before eclosion. Flies of genotype *UAS-*
1047 *RFP, UAS-flp, ubi>stop>GFP / +; bond-GAL4/ tub-GAL80(ts)* were dissected on the day of eclosion.
1048

1049 **Inferring clone types, FSC and EC numbers in newly-eclosed adults from scoring 2d-old**
1050 **adults**

1051 In order to make quantitative conclusions about the developmental process up to eclosion from scoring
1052 clonal outcomes in 2d-old adults we made the following assumptions and adjustments. We assumed
1053 that EC numbers and locations did not change during this 2d interval because ECs generally appear to
1054 be quite long-lived. ECs are, however, produced from FSCs during adulthood, so it is likely that a small
1055 number of marked ECs scored at +2d were produced from FSCs after eclosion. The proportion of

1056 marked ECs arising from FSCs is likely small based on known rates of FSC conversion to ECs [24, 40]
1057 and the observed high frequency of FSC clones with no ECs (44%) from -2d samples. Individual
1058 marked FSCs can be lost, mainly by becoming FCs, or amplified at high rates during adulthood [23]. If
1059 one or more marked FSCs were present at 0d but became an FC by +2d the resulting marked FCs
1060 would reside around the two germarial cysts or in the two youngest egg chambers because egg
1061 chambers bud roughly every 12h, allowing four cycles of FC recruitment over 2d. We therefore scored
1062 an ovariole as containing an FSC (classifying it as an FSC-only or FSC/EC lineage, according to EC
1063 content) if there were any marked FCs up to and including the second egg chamber, even if there were
1064 no FSCs at +2d. In those cases, we scored the number of marked FSCs as zero. On average, the
1065 number of marked FSCs should remain constant from 0d to +2d, so we should obtain a very good
1066 estimation of FSC numbers at 0d by scoring the numbers of marked FSCs at +2d, provided we include
1067 all examples where all marked FSCs were lost as containing zero FSCs. By using these guidelines, we
1068 could surmise the number of different types of clone at 0d and the number of constituent ECs and
1069 FSCs from data collected by scoring clones in 2d-old adults.
1070

1071 **Calculation of single-cell lineage frequencies assuming independent recombination**
1072 **events**

1073 The proportion of marked ovarioles with a lineage originating from a single marked cell is generally
1074 estimated by assuming that the probability of each dividing precursor to be labeled is independent. The
1075 estimate derives principally from the observed frequency of unlabeled ovarioles but it is also dependent
1076 to a small degree on the number of potential target cells. Different numbers of assumed target cells are
1077 used in the calculations below to demonstrate that estimated single cell frequencies are not greatly
1078 altered by this value.
1079 For the -6d to -2d time course, the average frequency of labeled ovarioles was about 60%.

1080 If there were, for example, only 6 target cells and we assume a binomial distribution (independent
1081 probabilities) of labeling, the chance of any one cell giving a clone is p and the chance of 6 cells not
1082 giving a clone is $(1-p)^6$. The observed no-clone fraction was 0.4, so (1-p)= 0.86 and p =0.14. Hence, the
1083 single clone frequency among 6 cells is $6p(1-p)^5$, and the frequency among labeled ovarioles is 1/0.6
1084 fold higher (because 60% were labeled). Therefore, the expected frequency of single-cell lineages is
1085 $6x0.14x(0.86)^5/0.6= 0.66$.
1086 If there were instead 15 target cells then p = 0.06 (because $0.94^{15}= 0.4$) and the frequency of single-cell
1087 lineages is $15x0.06x(0.94)^{14}/0.6= 0.63$.
1088 If there were 30 target cells then p = 0.03 (because $0.97^{30}= 0.4$) and the frequency of single-cell
1089 lineages is $30x0.03x(0.97)^{29}/0.6= 0.62$.
1090 For the multicolor experiment examining newly-eclosed adults 5d after heat-shock, the
1091 frequency of labeled ovarioles was 26/115 = 23%. If there were 20 target cells (likely in the range of the
1092 actual number of precursors), then p = 0.013 (because $0.987^{20}= 0.77$) and the frequency of single-cell
1093 lineages is $20x0.013x(0.987)^{19}/0.23 = 0.86$.
1094 For the MARCM experiment examining newly-eclosed adults 5d after heat-shock, the frequency
1095 of labeled ovarioles was 33%. If there were 20 target cells, then p = 0.02 (because $0.98^{20}= 0.67$) and
1096 the frequency of single-cell lineages is $20x0.02x(0.98)^{19}/0.33 = 0.80$.
1097

1098 **Calculation of single-cell lineage frequencies assuming frequencies of single lineages**
1099 **based on the experimental frequency of ovarioles with marked ECs and FCs**

1100 In MARCM and multicolor lineage experiments scored in newly-eclosed adults we observed a higher
1101 frequency of ovarioles with labeled ECs and FCs but no FSCs (which we assume represent two distinct
1102 lineages because the marked cells are discontinuous) than would be expected based on the frequency
1103 of unmarked ovarioles and assuming all recombination events are independent. Based on the EC/FC
1104 clone frequency we used trial and error (using increments of 5%) to find the percentage of ovarioles

with a single lineage that best fit the entire data-set of clone type frequencies we observed, using the simplifying assumption that all other marked ovarioles harbored exactly two lineages. In reality, the proportion of ovarioles with single lineages may be slightly different and a few ovarioles may include three or more marked lineages but the simplifying approximations we used are likely to be close to reality. These calculations, presented below, are better approximations than are generally made by simply considering the proportion of ovarioles with no marked cells.

MARCM clones induced 5d (0h APF) before eclosion

Single cell lineage frequencies and labeled cell content were calculated after estimating that 30% of marked ovarioles derived from a single marked cell, while the remaining 70% derived from two marked cells. In all cases, EC/FSC and FSC-only categories include clones with and without FCs (aggregated). pEC, pEC/FSC, pFSC, pFC are the proportions of each type of single-cell lineage amongst all marked lineages. Observed values are the proportion of marked ovarioles with the specific type(s) of cell. EC-only means no FSC. FC-only means no FSC. Both categories include EC+FC ovarioles.

Observed EC-only = 0.47 + 0.16 (with FCs) = 0.63 = 0.3 pEC + 0.7 $(pEC)^2$ + 1.4pEC.pFC

Observed FC-only = 0.09 + 0.16 = 0.25 = 0.3 pFC + 0.7 $(pFC)^2$ + 1.4pEC.pFC

Above is satisfied by pEC = 0.63 and pFC = 0.19

Observed FSC-only = 0.03 = 0.3pFSC + 0.7 [$(pFSC)^2$ + 2pFSC.pFC]

= 0.7[$(pFSC)^2$ + 0.566pFSC

So, pFSC = 0.050

Hence, pEC/FSC = 1 – (pEC + pFSC + pFC) = 0.13

The above values are the inferred single lineage frequencies of different types. The number of marked ECs and FSCs in each category is then deduced from these proportions and the observed number of marked cells in different types of marked ovariole.

Observed ECs per EC-only ovariole = (2.4 x0.47 + 2.9 x 0.16)/ 0.63 = 2.53

Of double-clones in EC-only, 0.397/0.636= 0.624 are deduced from clone type proportions to be two EC clones and 0.239/0.636 = 0.376 are one EC and one FC clone

So, number of EC lineages per EC-only ovariole = 0.3 + 0.7(1.248 + 0.376) = 1.44

So ECs per EC-only lineage = 2.53/1.44 =1.76

Observed FSCs per FSC-only ovariole = 14/3

Of double-clones in FSC-only, 0.0025/0.215= 0.116 are two FSC clones and 0.019/0.215 = 0.884 are one FSC and one FC clone

So, number of FSC lineages per FSC-only ovariole = 0.3 + 0.7(0.232 + 0.884) = 1.08

So FSCs per FSC-only lineage = 14/(3x1.08) = 4.32

Total ovarioles with marked cells= 98, so total number of lineages= 98 x 1.7 = 166.6

Total ECs from EC-only lineages = 166.6pEC(1.76) = 184.7

Total FSCs from FSC-only lineages = 166.6pFSC(4.32) = 35.9

Total ECs scored = 253, total FSCs scored = 111

So, total ECs from EC/FSC clones = 68.3

Total FSCs from EC/FSC clones = 75.1

Total EC/FSC lineages = 166.6pEC/FSC = 21.66

So, ECs per EC/FSC clone = 3.15, and FSCs per EC/FSC clone = 3.47

Deduced 24.0 precursors (to produce 16 FSCs): 15.1 pECs, 3.1 pEC/FSCs, 1.2 pFSCs, 4.6 pFCs.

Multicolor clones induced 5d (0h APF) before eclosion

Analogous calculations for multicolor GFP-only clones where EC plus FC category was 8% and we consequently assume that 70% of marked ovarioles have lineages derived from one cell, and 30% have two lineages.

Observed EC-only = 0.423 + 0.077 = 0.50 = 0.7 pEC + 0.3 $(pEC)^2$ + 0.6pEC.pFC

Observed FC-only = 0.077 + 0.077 = 0.154 = 0.7 pFC + 0.3 $(pFC)^2$ + 0.6pEC.pFC

Above satisfied by pEC= 0.52 and pFC= 0.14

Observed FSC-only = 0.077 = 0.7pFSC + 0.3 $[(pFSC)^2$ + 2pFSC.pFC]

= 0.3$[(pFSC)^2$ + 0.778pFSC

So, pFSC = 0.095

Hence, pEC/FSC = 1 – (pEC + pFSC + pFC) = 0.245

The above values are the inferred single lineage frequencies of different types. The number of marked ECs and FSCs in each category is then deduced from these proportions and the observed number of marked cells in different types of marked ovariole.

Observed ECs per EC-only ovariole = 38/13 = 2.92

Of double-clones in EC-only, 0.2704/0.416 = 0.65 are two EC clones and 0.1456/0.416 = 0.35 are one EC and one FC clone

So, number of EC lineages per EC-only ovariole = 0.7 + 0.3(1.3 + 0.35) = 1.195

So ECs per EC-only lineage = 2.92/1.195 = 2.44

Observed FSCs per FSC-only ovariole = 4.0

Of double-clones in FSC-only, 0.00593/0.02363= 0.25 are two FSC clones and 0.0177/0.02363= 0.75 are one FSC and one FC clone

So, number of lineages per FSC-only ovariole = 0.7 + 0.3(0.50 + 0.75) = 1.0375

So FSCs per FSC-only lineage = 4.0/1.0375 = 3.86

Total ovarioles with marked cells= 26, so total number of lineages= 26 x 1.3 = 33.8

Total ECs from EC-only lineages = 33.8pEC(2.44) = 42.89

Total FSCs from FSC-only lineages = 33.8pFSC(3.86) = 10.04

Total ECs scored = 66, total FSCs scored = 29

So, total ECs from EC/FSC clones = 23.11

Total FSCs from EC/FSC clones = 18.96

Total EC/FSC lineages = 33.8pEC/FSC = 8.28

1183 So, ECs per EC/FSC clone = 2.79, and FSCs per EC/FSC clone = 2.27

1184

1185 Deduced 17.3 precursors (to produce 16 FSCs): 9.0pECs, 4.2 pEC/FSCs, 1.6 pFSCs, 2.0 pFCs.

1186

1187 *MARCM clones induced 3.5d (36h APF) before eclosion*

1188 Analogous calculations for MARCM clones induced at -3.5d, where EC plus FC category was 44% and

1189 assuming all marked ovarioles have two lineages.

1190

1191 Observed EC-only = 0.207 + 0.438 = 0.645 = $(pEC)^2 + 2pEC.pFC$

1192 Observed FC-only = 0.091 + 0.438 = 0.529 = $(pFC)^2 + 2pEC.pFC$

1193 Above satisfied by pEC= 0.51 and pFC= 0.38

1194 Observed FSC-only = 0.033 = $(pFSC)^2 + 2pFSC.pFC = (pFSC)^2 + 0.76pFSC$

1195 So, pFSC = 0.041

1196 Hence, pEC/FSC = 1 – (pEC + pFSC + pFC) = 0.07

1197 The above values are the inferred single lineage frequencies of different types. The number of marked

1198 ECs and FSCs in each category is then deduced from these proportions and the observed number of

1199 marked cells in different types of marked ovariole.

1200 Of double-clones in FC-only, 0.144/0.532= 0.27 are two FC clones and 0.388/0.532 = 0.73 are one EC

1201 and one FC clone

1202 Observed ECs per EC-only ovariole = 199/78 = 2.55

1203 Of double-clones in EC-only, 0.260/0.646= 0.40 are two EC clones and 0.388/0.646 = 0.60 are one EC

1204 and one FC clone

1205 So, number of EC lineages per EC-only ovariole = 0.8 + 0.6 = 1.40

1206 So, ECs per EC-only lineage = 2.55/1.40 =1.82

1207 Observed FSCs per FSC-only ovariole = 13/4 = 3.25

1208 Of double-clones in FSC-only, 0.00168/0.03284= 0.05 are two FSC clones and 0.03116/0.03284= 0.95

1209 are one FSC and one FC clone

1210 So, number of FSC-only lineages per FSC-only ovariole = 1.05

1211 So, FSCs per FSC-only lineage = 3.25/1.05 = 3.10

1212

1213 Total ovarioles with marked cells= 121, so total number of lineages= 242

1214 Total ECs from EC-only lineages = 242pEC(1.82) = 224.6

1215 Total FSCs from FC-only lineages = 242pFSC(3.10) = 30.8

1216 Total ECs scored = 276, total FSCs scored = 111

1217 So, total ECs from EC/FSC clones = 51.4

1218 Total FSCs from EC/FSC clones = 80.2

1219 Total EC/FSC lineages = 242pEC/FSC = 16.94

1220 So ECs per EC/FSC clone = 3.03, and FSCs per EC/FSC clone = 4.73

1221

1222 Deduced 34.9 precursors (to produce 16 FSCs): 17.8pECs, 2.4 pEC/FSCs, 1.4 pFSCs, 13.3 pFCs.

1223 Also, by this time there are EC precursors that no longer divide (estimated at 5 for -4d and 18 for -3d

1224 from MARCM lineages examined in +2d adults, so perhaps 11.5 at -3.5d, to give a total of 45.4

1225 precursors. So, estimated proportion of precursors that are pFCs is 13.3/45.4 = 29%.

1226

1227 *bond-GAL4/G-trace lineages*

1228 Single lineage frequencies and content for clones initiated by *bond-GAL4* were calculated in a slightly

1229 different way (considering ovarioles with only marked ECs to calculate EC-only single lineage and then

1230 ovarioles with labeled ECs and FCs clones to calculate the FC-only lineage frequency) because there

1231 were almost no ovarioles with only marked FCs.

1232 Here we assumed that every labeled ovariole had exactly two lineages.

1233 Observed EC frequency = 38.36% = $(pEC)^2$

1234 So, pEC= 61.9%

1235 Observed EC+FC frequency= 9.59% = 2pEC.pFC

1236 So, pFC = 7.75%

1237 Observed FSC frequency = 1.37% = $(pFC)^2$ + 2pFC. pFSC

1238 So, pFSC= 6.29%

1239 Therefore pEC/FSC = 24.0%

1240 Observed EC per EC-only (or EC+FC) lineage= 207/35= 5.91

1241 Of double-clones in EC-only, expected frequencies: 0.383/0.479= 0.80 are two EC clones and

1242 0.096/0.479 = 0.20 are one EC and one FC clone

1243 So, number of EC lineages per EC-only ovariole = 2x 0.8 + 0.2= 1.8

1244 So, ECs per EC-only lineage = 5.91/1.8 =3.28

1245 Ovariole with labeled FSCs but no ECs has 7 FSCs

1246 Of double-clones in FSC-only, 0.00396/0.01371= 0.289 are two FSC clones and 0.00975/0.01371 =

1247 0.721 are one FSC and one FC clone

1248 So, number of FSC lineages per FSC-only ovariole = 2x0.289 + 0.721 = 1.32

1249 So, FSCs per FSC-only lineage = 7/1.32 = 5.3

1250

1251 Total ovarioles with marked cells= 73, so total number of lineages= 146

1252 Total ECs from EC-only lineages = 146pEC(3.28) = 296.4

1253 Total FSCs from FSC-only lineages = 146pFSC(5.3) = 48.7

1254 Total ECs scored = 496, total FSCs scored = 190

1255 So, total ECs from EC/FSC clones = 199.6

1256 Total FSCs from EC/FSC clones = 141.3

1257 Total EC/FSC lineages = 146pEC/FSC = 35.4

1258 So, ECs per EC/FSC clone = 5.64, and FSCs per EC/FSC clone = 3.99

1259

1260 **Table 1. Frequency of clones originating from different precursors and yields per clone.**

1261

Heat-shock to eclosion (days)	pr1 ECs		pr1/2a ECs			pEC/FSC				pFSC	
	Freq.	Yield	Freq.	Yield		Freq.	Yield			Freq.	Yield
	%	r1	%	r1	r2a	%	r1	r2a	FSC	%	FSC
2	7.9	1.2	6.3	0.3	1.8	41	0.5	1.2	1.3	44	1.2
3	14	1.2	16	0.8	2.2	40	0.9	1	2.6	30	1.4
4	34	2.1	23	2	1.6	38	1.6	1.5	3.7	4.6	3
5	33	2.2	25	2.8	2.3	40	3.1	3.4	5.5	2.7	2.5
6	31	3.5	14	3.3	3.6	53	3.2	3.4	4.8	2.7	3

1262

1263

1264

1265

1266 **Table 2. Number of adult cells of each type made from dividing precursors at different**

1267 **developmental times calculated from the total yield of marked cells of each type.**

1268

Heat-shock to eclosion (days)	Total Number of marked cells in clones				Cells made per germarium from dividing precursors			
	r1	r2a	EC	FSC	r1	r2a	EC	FSC
	x	y	x+y	z	16x/z	16y/z	16(x+y)/z	
2	20	37	57	69	4.6	8.6	13.2	16
3	41	46	87	93	7.1	7.9	15	16
4	156	80	236	134	18.6	9.6	28.2	16
5	191	140	331	164	18.6	13.7	32.3	16
6	356	253	609	295	19.3	13.7	33	16

1269

1270

1271

	n	EC		EC/FSC			FSC		FC	EC+FC		Number of dividing precursors per germarium				
		Freq.	Yield	Freq.	Yield		Freq.	Yield	Freq.	Freq.	Yield	Total (n)	pEC	pEC/FSC	pFSC	pFC
		%	EC	%	EC	FSC	%	FSC	%	%	EC					
		100p		100q		x	100r	y	100s			16/ (qx+ry)	pn	qn	rn	sn
0h APFMARCM raw data	98	46.9	2.4	25	4	4	3	4.3	9.2	16.3	2.9					
0h APF MARCM assuming 70% double clones		63	1.8	13	3.2	3.5	5	4.3	19			24	15.1	3.1	1.2	4.6
0h APF Mulicolor raw data	26	42.3	3	31	3.5	2.6	7.7	4	12	7.7	2.5					
0h APF Multicolor assuming 30% double clones		52	2.4	25	2.1	2.3	9.5	3.9	14			17.3	9	4.2	1.6	2.4
36h APF MARCM raw data	121	20.7	2.5	23	2.8	3.5	3.3	3.3	9.1	43.8	2.6					
36h APF MARCM assuming all double clones		51	1.8	7	3	4.7	4.1	3.1	38			34.9	17.8	2.4	1.4	13
bond-GAL4 raw data	73	38.4	5.1	48	8.3	5.4	1.4	7	2.7	9.6	9					
bond-GAL4 assuming all double clones		61.9	3.3	24	5.6	4	6.3	5.3	7.8			15.1	9.4	3.6	1	1.2

1272

1273 **Table 3. Clone frequencies and cellular yields from different lineage experiments together with**

1274 **deduced single-lineage parameters including the number of precursors of different types.**

References

1. Clevers H, Watt FM. Defining Adult Stem Cells by Function, not by Phenotype. Annu Rev Biochem. 2018;87:1015-27. doi: 10.1146/annurev-biochem-062917-012341. PubMed PMID: 29494240.
2. Post Y, Clevers H. Defining Adult Stem Cell Function at Its Simplest: The Ability to Replace Lost Cells through Mitosis. Cell Stem Cell. 2019;25(2):174-83. doi: 10.1016/j.stem.2019.07.002. PubMed PMID: 31374197.
3. Biteau B, Hochmuth CE, Jasper H. Maintaining tissue homeostasis: dynamic control of somatic stem cell activity. Cell Stem Cell. 2011;9(5):402-11. Epub 2011/11/08. doi: 10.1016/j.stem.2011.10.004. PubMed PMID: 22056138; PubMed Central PMCID: PMCPMC3212030.
4. Losick VP, Morris LX, Fox DT, Spradling A. Drosophila stem cell niches: a decade of discovery suggests a unified view of stem cell regulation. Dev Cell. 2011;21(1):159-71. Epub 2011/07/19. doi: S1534-5807(11)00252-8 [pii]
10.1016/j.devcel.2011.06.018. PubMed PMID: 21763616.
5. Voog J, Jones DL. Stem cells and the niche: a dynamic duo. Cell Stem Cell. 2010;6(2):103-15. Epub 2010/02/11. doi: 10.1016/j.stem.2010.01.011. PubMed PMID: 20144784; PubMed Central PMCID: PMCPMC3012646.
6. Akbari S, Arslan N, Senturk S, Erdal E. Next-Generation Liver Medicine Using Organoid Models. Front Cell Dev Biol. 2019;7:345. doi: 10.3389/fcell.2019.00345. PubMed PMID: 31921856; PubMed Central PMCID: PMCPMC6933000.
7. Merenda A, Fenderico N, Maurice MM. Wnt Signaling in 3D: Recent Advances in the Applications of Intestinal Organoids. Trends Cell Biol. 2020;30(1):60-73. doi: 10.1016/j.tcb.2019.10.003. PubMed PMID: 31718893.
8. Petersen MBK, Goncalves CAC, Kim YH, Grapin-Botton A. Recapitulating and Deciphering Human Pancreas Development From Human Pluripotent Stem Cells in a Dish. Current topics in developmental biology. 2018;129:143-90. doi: 10.1016/bs.ctdb.2018.02.009. PubMed PMID: 29801529.
9. Pourquie O, Al Tanoury Z, Chal J. The Long Road to Making Muscle In Vitro. Current topics in developmental biology. 2018;129:123-42. doi: 10.1016/bs.ctdb.2018.03.003. PubMed PMID: 29801528.
10. Yousef Yengej FA, Jansen J, Rookmaaker MB, Verhaar MC, Clevers H. Kidney Organoids and Tubuloids. Cells. 2020;9(6). doi: 10.3390/cells9061326. PubMed PMID: 32466429.
11. Drost J, Clevers H. Translational applications of adult stem cell-derived organoids. Development. 2017;144(6):968-75. doi: 10.1242/dev.140566. PubMed PMID: 28292843.

1307 12. Adam MA, Harwell CC. Epigenetic regulation of cortical neurogenesis; orchestrating fate
1308 switches at the right time and place. Curr Opin Neurobiol. 2020;63:146-53. doi:
1309 10.1016/j.conb.2020.03.012. PubMed PMID: 32428815.
1310 13. Davidson EH, Rast JP, Oliveri P, Ransick A, Calestani C, Yuh CH, et al. A genomic regulatory
1311 network for development. Science. 2002;295(5560):1669-78. doi: 10.1126/science.1069883. PubMed
1312 PMID: 11872831.
1313 14. Rothman J, Jarriault S. Developmental Plasticity and Cellular Reprogramming in Caenorhabditis
1314 elegans. Genetics. 2019;213(3):723-57. doi: 10.1534/genetics.119.302333. PubMed PMID: 31685551;
1315 PubMed Central PMCID: PMCPMC6827377.
1316 15. Sagner A, Briscoe J. Establishing neuronal diversity in the spinal cord: a time and a place.
1317 Development. 2019;146(22). doi: 10.1242/dev.182154. PubMed PMID: 31767567.
1318 16. Salinas RD, Connolly DR, Song H. Invited Review: Epigenetics in neurodevelopment.
1319 Neuropathol Appl Neurobiol. 2020;46(1):6-27. doi: 10.1111/nan.12608. PubMed PMID: 32056273;
1320 PubMed Central PMCID: PMCPMC7174139.
1321 17. Zechner C, Nerli E, Norden C. Stochasticity and determinism in cell fate decisions.
1322 Development. 2020;147(14). doi: 10.1242/dev.181495. PubMed PMID: 32669276.
1323 18. Donati G, Watt FM. Stem cell heterogeneity and plasticity in epithelia. Cell Stem Cell.
1324 2015;16(5):465-76. doi: 10.1016/j.stem.2015.04.014. PubMed PMID: 25957902.
1325 19. Tetteh PW, Farin HF, Clevers H. Plasticity within stem cell hierarchies in mammalian epithelia.
1326 Trends Cell Biol. 2015;25(2):100-8. doi: 10.1016/j.tcb.2014.09.003. PubMed PMID: 25308311.
1327 20. Wabik A, Jones PH. Switching roles: the functional plasticity of adult tissue stem cells. EMBO J.
1328 2015;34(9):1164-79. doi: 10.15252/embj.201490386. PubMed PMID: 25812989; PubMed Central
1329 PMCID: PMCPMC4426478.
1330 21. Gehart H, Clevers H. Tales from the crypt: new insights into intestinal stem cells. Nat Rev
1331 Gastroenterol Hepatol. 2019;16(1):19-34. doi: 10.1038/s41575-018-0081-y. PubMed PMID: 30429586.
1332 22. Hayashi Y, Yoshinari Y, Kobayashi S, Niwa R. The regulation of Drosophila ovarian stem cell
1333 niches by signaling crosstalk. Curr Opin Insect Sci. 2020;37:23-9. doi: 10.1016/j.cois.2019.10.006.
1334 PubMed PMID: 32087560.
1335 23. Reilein A, Melamed D, Park KS, Berg A, Cimetta E, Tandon N, et al. Alternative direct stem cell
1336 derivatives defined by stem cell location and graded Wnt signalling. Nat Cell Biol. 2017;19(5):433-44.
1337 doi: 10.1038/ncb3505. PubMed PMID: 28414313.
1338 24. Melamed D, Kalderon D. Opposing JAK-STAT and Wnt signaling gradients define a stem cell
1339 domain by regulating differentiation at two borders. Elife. 2020;9. Epub 2020/11/03. doi:
1340 10.7554/eLife.61204. PubMed PMID: 33135631; PubMed Central PMCID: PMCPMC7695452.

1341 25. Song X, Xie T. Wingless signaling regulates the maintenance of ovarian somatic stem cells in
1342 Drosophila. Development. 2003;130(14):3259-68.
1343 26. Vied C, Reilein A, Field NS, Kalderon D. Regulation of stem cells by intersecting gradients of
1344 long-range niche signals. Dev Cell. 2012;23(4):836-48. Epub 2012/10/20. doi:
1345 10.1016/j.devcel.2012.09.010. PubMed PMID: 23079600; PubMed Central PMCID: PMC3479678.
1346 27. Waghmare I, Page-McCaw A. Wnt Signaling in Stem Cell Maintenance and Differentiation in the
1347 Drosophila Germarium. Genes (Basel). 2018;9(3). doi: 10.3390/genes9030127. PubMed PMID:
1348 29495453; PubMed Central PMCID: PMCPMC5867848.
1349 28. Beumer J, Clevers H. Cell fate specification and differentiation in the adult mammalian intestine.
1350 Nature reviews Molecular cell biology. 2020. Epub 2020/09/23. doi: 10.1038/s41580-020-0278-0.
1351 PubMed PMID: 32958874.
1352 29. Hsu YC, Fuchs E. A family business: stem cell progeny join the niche to regulate homeostasis.
1353 Nature reviews Molecular cell biology. 2012;13(2):103-14. Epub 2012/01/24. doi: 10.1038/nrm3272.
1354 PubMed PMID: 22266760; PubMed Central PMCID: PMC3280338.
1355 30. Fuchs E, Blau HM. Tissue Stem Cells: Architects of Their Niches. Cell Stem Cell.
1356 2020;27(4):532-56. Epub 2020/10/03. doi: 10.1016/j.stem.2020.09.011. PubMed PMID: 33007238.
1357 31. Kahney EW, Snedeker JC, Chen X. Regulation of Drosophila germline stem cells. Curr Opin
1358 Cell Biol. 2019;60:27-35. doi: 10.1016/j.ceb.2019.03.008. PubMed PMID: 31014993; PubMed Central
1359 PMCID: PMCPMC6756965.
1360 32. Gilboa L. Organizing stem cell units in the Drosophila ovary. Curr Opin Genet Dev. 2015;32:31-
1361 6. doi: 10.1016/j.gde.2015.01.005. PubMed PMID: 25703842.
1362 33. Kirilly D, Wang S, Xie T. Self-maintained escort cells form a germline stem cell differentiation
1363 niche. Development. 2011;138(23):5087-97. Epub 2011/10/28. doi: 10.1242/dev.067850. PubMed
1364 PMID: 22031542; PubMed Central PMCID: PMC3210492.
1365 34. Sahai-Hernandez P, Nystul TG. A dynamic population of stromal cells contributes to the follicle
1366 stem cell niche in the Drosophila ovary. Development. 2013;140(22):4490-8. doi: 10.1242/dev.098558.
1367 PubMed PMID: 24131631; PubMed Central PMCID: PMCPMC3817939.
1368 35. Wang X, Page-McCaw A. Wnt6 maintains anterior escort cells as an integral component of the
1369 germline stem cell niche. Development. 2018;145(3). doi: 10.1242/dev.158527. PubMed PMID:
1370 29361569; PubMed Central PMCID: PMCPMC5818006.
1371 36. Zhang Y, Kalderon D. Hedgehog acts as a somatic stem cell factor in the Drosophila ovary.
1372 Nature. 2001;410(6828):599-604.

1373 37. Duhart JC, Parsons TT, Raftery LA. The repertoire of epithelial morphogenesis on display:
1374 Progressive elaboration of Drosophila egg structure. Mech Dev. 2017;148:18-39. doi:
1375 10.1016/j.mod.2017.04.002. PubMed PMID: 28433748.
1376 38. McGregor JR, Xi R, Harrison DA. JAK signaling is somatically required for follicle cell
1377 differentiation in Drosophila. Development. 2002;129(3):705-17. Epub 2002/02/07. PubMed PMID:
1378 11830571.
1379 39. Xi R, McGregor JR, Harrison DA. A gradient of JAK pathway activity patterns the anterior-
1380 posterior axis of the follicular epithelium. Developmental Cell. 2003;4(2):167-77.
1381 40. Reilein A, Melamed D, Tavare S, Kalderon D. Division-independent differentiation mandates
1382 proliferative competition among stem cells. Proc Natl Acad Sci U S A. 2018;115(14):E3182-E91. doi:
1383 10.1073/pnas.1718646115. PubMed PMID: 29555768; PubMed Central PMCID: PMCPMC5889645.
1384 41. Vied C, Kalderon D. Hedgehog-stimulated stem cells depend on non-canonical activity of the
1385 Notch co-activator Mastermind. Development. 2009;136(13):2177-86. Epub 2009/05/29. doi:
1386 dev.035329 [pii]
1387 10.1242/dev.035329. PubMed PMID: 19474148.
1388 42. Wang X, LaFever KS, Waghmare I, Page-McCaw A. Extracellular spreading of Wingless is
1389 required for Drosophila oogenesis. PLoS Genet. 2021;17(4):e1009469. Epub 2021/04/03. doi:
1390 10.1371/journal.pgen.1009469. PubMed PMID: 33798197.
1391 43. Jemc JC. Somatic gonadal cells: the supporting cast for the germline. Genesis.
1392 2011;49(10):753-75. doi: 10.1002/dvg.20784. PubMed PMID: 21735540.
1393 44. Murray SM, Yang SY, Van Doren M. Germ cell sex determination: a collaboration between
1394 soma and germline. Curr Opin Cell Biol. 2010;22(6):722-9. doi: 10.1016/j.ceb.2010.09.006. PubMed
1395 PMID: 21030233; PubMed Central PMCID: PMCPMC2996260.
1396 45. Godt D, Laski FA. Mechanisms of cell rearrangement and cell recruitment in Drosophila ovary
1397 morphogenesis and the requirement of bric a brac. Development. 1995;121(1):173-87.
1398 46. Cohen ED, Mariol MC, Wallace RM, Weyers J, Kamberov YG, Pradel J, et al. DWnt4 regulates
1399 cell movement and focal adhesion kinase during Drosophila ovarian morphogenesis. Dev Cell.
1400 2002;2(4):437-48. doi: 10.1016/s1534-5807(02)00142-9. PubMed PMID: 11970894.
1401 47. Irizarry J, Stathopoulos A. FGF signaling supports Drosophila fertility by regulating development
1402 of ovarian muscle tissues. Developmental biology. 2015;404(1):1-13. doi: 10.1016/j.ydbio.2015.04.023.
1403 PubMed PMID: 25958090; PubMed Central PMCID: PMCPMC4469552.
1404 48. King RC, Aggarwal SK, Aggarwal U. The development of the female Drosophila reproductive
1405 system. J Morphol. 1968;124(2):143-66. doi: 10.1002/jmor.1051240203. PubMed PMID: 5654408.

1406 49. Valer FB, Machado MCR, Silva-Junior RMP, Ramos RGP. Expression of Hbs, Kirre, and Rst
1407 during Drosophila ovarian development. Genesis. 2018;56(9):e23242. doi: 10.1002/dvg.23242.
1408 PubMed PMID: 30114331.
1409 50. Park KS, Godt D, Kalderon D. Dissection and Staining of Drosophila Pupal Ovaries. Journal of
1410 visualized experiments : JoVE. 2018;(133). doi: 10.3791/56779. PubMed PMID: 29553514; PubMed
1411 Central PMCID: PMCPMC5931425.
1412 51. Slaidina M, Banisch TU, Gupta S, Lehmann R. A single-cell atlas of the developing Drosophila
1413 ovary identifies follicle stem cell progenitors. Genes Dev. 2020;34(3-4):239-49. doi:
1414 10.1101/gad.330464.119. PubMed PMID: 31919193; PubMed Central PMCID: PMCPMC7000915.
1415 52. Lai CM, Lin KY, Kao SH, Chen YN, Huang F, Hsu HJ. Hedgehog signaling establishes
1416 precursors for germline stem cell niches by regulating cell adhesion. J Cell Biol. 2017;216(5):1439-53.
1417 doi: 10.1083/jcb.201610063. PubMed PMID: 28363970; PubMed Central PMCID: PMCPMC5412570.
1418 53. Li M, Hu X, Zhang S, Ho MS, Wu G, Zhang L. Traffic jam regulates the function of the ovarian
1419 germline stem cell progeny differentiation niche during pre-adult stage in Drosophila. Sci Rep.
1420 2019;9(1):10124. doi: 10.1038/s41598-019-45317-6. PubMed PMID: 31300663; PubMed Central
1421 PMCID: PMCPMC6626045.
1422 54. Panchal T, Chen X, Alchits E, Oh Y, Poon J, Kouptsova J, et al. Specification and spatial
1423 arrangement of cells in the germline stem cell niche of the Drosophila ovary depend on the Maf
1424 transcription factor Traffic jam. PLoS Genet. 2017;13(5):e1006790. doi: 10.1371/journal.pgen.1006790.
1425 PubMed PMID: 28542174; PubMed Central PMCID: PMCPMC5459507.
1426 55. Sahut-Barnola I, Dastugue B, Couderc JL. Terminal filament cell organization in the larval ovary
1427 of Drosophila melanogaster: ultrastructural observations and pattern of divisions. Roux Arch Dev Biol.
1428 1996;205(7-8):356-63. doi: 10.1007/BF00377215. PubMed PMID: 28306086.
1429 56. Banisch TU, Slaidina M, Gupta S, Gilboa L, Lehmann R. A transitory signaling center controls
1430 timing of primordial germ cell differentiation. bioRxiv. 2020:2020.08.01.232298. doi:
1431 10.1101/2020.08.01.232298.
1432 57. Vlachos S, Jangam S, Conder R, Chou M, Nystul T, Harden N. A Pak-regulated cell
1433 intercalation event leading to a novel radial cell polarity is involved in positioning of the follicle stem cell
1434 niche in the Drosophila ovary. Development. 2015;142(1):82-91. doi: 10.1242/dev.111039. PubMed
1435 PMID: 25516970; PubMed Central PMCID: PMCPMC6514404.
1436 58. Diaz-Torres A, Rosales-Nieves AE, Pearson JR, Santa-Cruz Mateos C, Marin-Menguiano M,
1437 Marshall OJ, et al. Stem cell niche organization in the Drosophila ovary requires the ECM component
1438 Perlecan. Curr Biol. 2021. Epub 2021/02/24. doi: 10.1016/j.cub.2021.01.071. PubMed PMID:
1439 33621481.

1440 59. Gancz D, Gilboa L. Insulin and Target of rapamycin signaling orchestrate the development of
1441 ovarian niche-stem cell units in Drosophila. Development. 2013;140(20):4145-54. doi:
1442 10.1242/dev.093773. PubMed PMID: 24026119.
1443 60. Gancz D, Lengil T, Gilboa L. Coordinated regulation of niche and stem cell precursors by
1444 hormonal signaling. PLoS biology. 2011;9(11):e1001202. doi: 10.1371/journal.pbio.1001202. PubMed
1445 PMID: 22131903; PubMed Central PMCID: PMCPMC3222635.
1446 61. Song X, Call GB, Kirilly D, Xie T. Notch signaling controls germline stem cell niche formation in
1447 the Drosophila ovary. Development. 2007;134(6):1071-80. Epub 2007/02/09. doi: dev.003392 [pii]
1448 10.1242/dev.003392. PubMed PMID: 17287246.
1449 62. Yatsenko AS, Shcherbata HR. Stereotypical architecture of the stem cell niche is
1450 spatiotemporally established by miR-125-dependent coordination of Notch and steroid signaling.
1451 Development. 2018;145(3). doi: 10.1242/dev.159178. PubMed PMID: 29361571; PubMed Central
1452 PMCID: PMCPMC5818007.
1453 63. Asaoka M, Lin H. Germline stem cells in the Drosophila ovary descend from pole cells in the
1454 anterior region of the embryonic gonad. Development. 2004;131(20):5079-89.
1455 64. Zhu CH, Xie T. Clonal expansion of ovarian germline stem cells during niche formation in
1456 Drosophila. Development. 2003;130(12):2579-88.
1457 65. Deng W, Lin H. Spectrosomes and fusomes anchor mitotic spindles during asymmetric germ
1458 cell divisions and facilitate the formation of a polarized microtubule array for oocyte specification in
1459 Drosophila. Developmental biology. 1997;189(1):79-94.
1460 66. Golic KG, Lindquist S. The FLP recombinase of yeast catalyzes site-specific recombination in
1461 the Drosophila genome. Cell. 1989;59(3):499-509. doi: 10.1016/0092-8674(89)90033-0. PubMed
1462 PMID: 2509077.
1463 67. Lee T, Luo L. Mosaic analysis with a repressible cell marker (MARCM) for Drosophila neural
1464 development.[erratum appears in Trends Neurosci 2001 Jul;24(7):385]. Trends in Neurosciences.
1465 2001;24(5):251-4.
1466 68. Margolis J, Spradling A. Identification and behavior of epithelial stem cells in the Drosophila
1467 ovary. Development. 1995;121(11):3797-807.
1468 69. Li MA, Alls JD, Avancini RM, Koo K, Godt D. The large Maf factor Traffic Jam controls gonad
1469 morphogenesis in Drosophila. Nat Cell Biol. 2003;5(11):994-1000. doi: 10.1038/ncb1058. PubMed
1470 PMID: 14578908.
1471 70. Reilein A, Cimetta E, Tandon NM, Kalderon D, Vunjak-Novakovic G. Live imaging of stem cells
1472 in the germarium of the Drosophila ovary using a reusable gas-permeable imaging chamber. Nature

1473 protocols. 2018;13(11):2601-14. doi: 10.1038/s41596-018-0054-1. PubMed PMID: 30349048; PubMed
1474 Central PMCID: PMCPMC6314018.
1475 71. Zielke N, Korzelius J, van Straaten M, Bender K, Schuhknecht GF, Dutta D, et al. Fly-FUCCI: A
1476 versatile tool for studying cell proliferation in complex tissues. Cell Rep. 2014;7(2):588-98. doi:
1477 10.1016/j.celrep.2014.03.020. PubMed PMID: 24726363.
1478 72. Buckingham ME, Meilhac SM. Tracing cells for tracking cell lineage and clonal behavior. Dev
1479 Cell. 2011;21(3):394-409. Epub 2011/09/17. doi: 10.1016/j.devcel.2011.07.019. PubMed PMID:
1480 21920310.
1481 73. Kretzschmar K, Watt FM. Lineage tracing. Cell. 2012;148(1-2):33-45. doi:
1482 10.1016/j.cell.2012.01.002. PubMed PMID: 22265400.
1483 74. Evans CJ, Olson JM, Ngo KT, Kim E, Lee NE, Kuoy E, et al. G-TRACE: rapid Gal4-based cell
1484 lineage analysis in Drosophila. Nature methods. 2009;6(8):603-5. doi: 10.1038/nmeth.1356. PubMed
1485 PMID: 19633663; PubMed Central PMCID: PMCPMC2754220.
1486 75. Shi J, Jin Z, Yu Y, Zhang Y, Yang F, Huang H, et al. A Progressive Somatic Cell Niche
1487 Regulates Germline Cyst Differentiation in the Drosophila Ovary. Curr Biol. 2021;31(4):840-52 e5. Epub
1488 2020/12/20. doi: 10.1016/j.cub.2020.11.053. PubMed PMID: 33340458.
1489 76. Tu R, Duan B, Song X, Chen S, Scott A, Hall K, et al. Multiple Niche Compartments Orchestrate
1490 Stepwise Germline Stem Cell Progeny Differentiation. Curr Biol. 2021;31(4):827-39 e3. Epub
1491 2020/12/29. doi: 10.1016/j.cub.2020.12.024. PubMed PMID: 33357404; PubMed Central PMCID:
1492 PMCPMC7904662.
1493 77. Berg DA, Su Y, Jimenez-Cyrus D, Patel A, Huang N, Morizet D, et al. A Common Embryonic
1494 Origin of Stem Cells Drives Developmental and Adult Neurogenesis. Cell. 2019;177(3):654-68 e15.
1495 Epub 2019/04/02. doi: 10.1016/j.cell.2019.02.010. PubMed PMID: 30929900; PubMed Central PMCID:
1496 PMCPMC6496946.
1497 78. Guiu J, Hannezo E, Yui S, Demharter S, Ulyanchenko S, Maimets M, et al. Tracing the origin of
1498 adult intestinal stem cells. Nature. 2019;570(7759):107-11. Epub 2019/05/17. doi: 10.1038/s41586-019-
1499 1212-5. PubMed PMID: 31092921; PubMed Central PMCID: PMCPMC6986928.
1500 79. Fuentealba LC, Rompani SB, Parraguez JI, Obernier K, Romero R, Cepko CL, et al. Embryonic
1501 Origin of Postnatal Neural Stem Cells. Cell. 2015;161(7):1644-55. Epub 2015/06/20. doi:
1502 10.1016/j.cell.2015.05.041. PubMed PMID: 26091041; PubMed Central PMCID: PMCPMC4475276.
1503 80. Furutachi S, Miya H, Watanabe T, Kawai H, Yamasaki N, Harada Y, et al. Slowly dividing neural
1504 progenitors are an embryonic origin of adult neural stem cells. Nature neuroscience. 2015;18(5):657-
1505 65. Epub 2015/03/31. doi: 10.1038/nn.3989. PubMed PMID: 25821910.

1506 81. Harris RE, Ashe HL. Cease and desist: modulating short-range Dpp signalling in the stem-cell
1507 niche. EMBO Rep. 2011;12(6):519-26. doi: 10.1038/embor.2011.80. PubMed PMID: 21546910;
1508 PubMed Central PMCID: PMCPMC3128284.
1509 82. Banisch TU, Maimon I, Dadosh T, Gilboa L. Escort cells generate a dynamic compartment for
1510 germline stem cell differentiation via combined Stat and Erk signalling. Development.
1511 2017;144(11):1937-47. doi: 10.1242/dev.143727. PubMed PMID: 28559239.
1512
1513

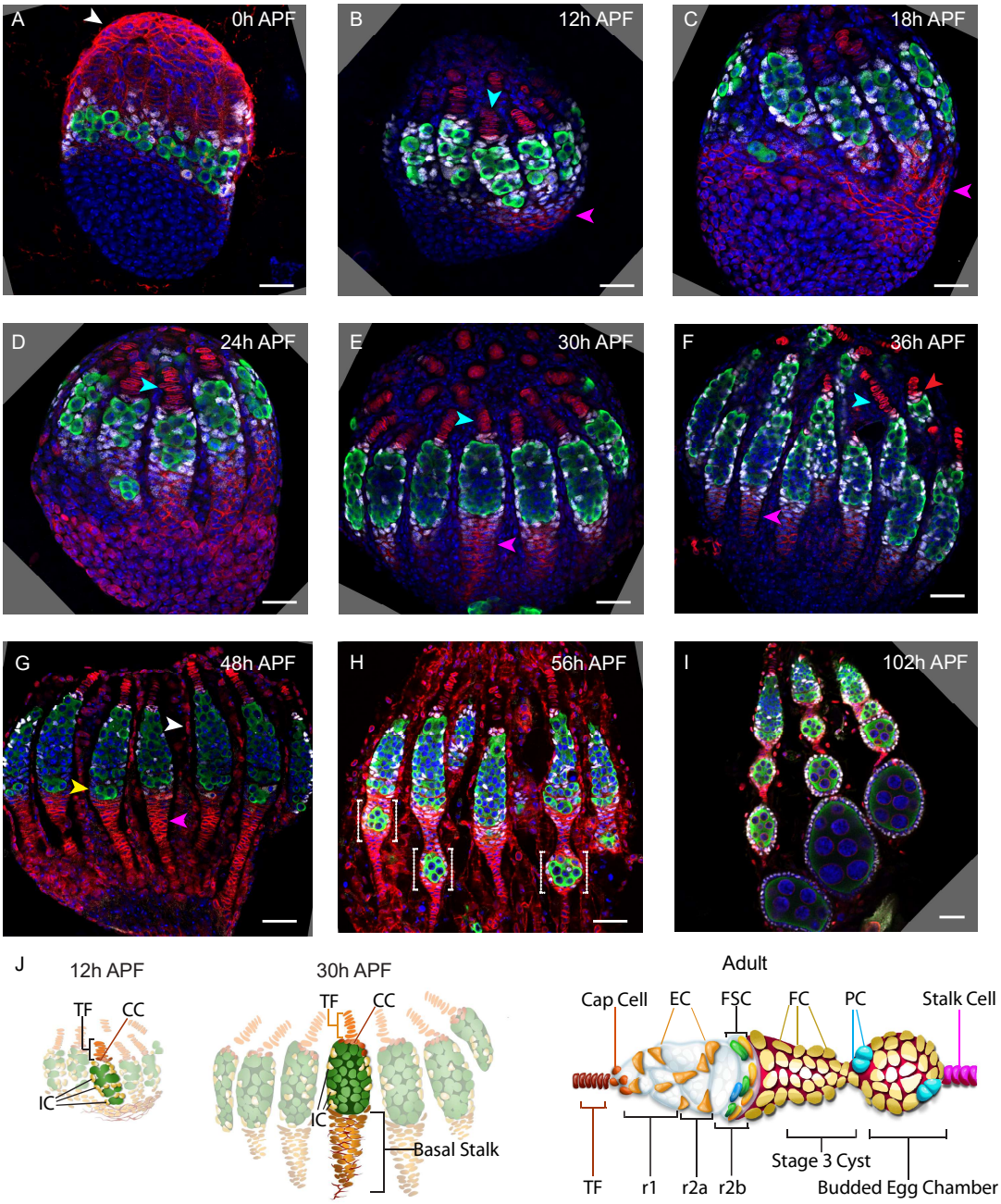

Figure 1. Development of adult germaria during early pupal stages.

(A-J) A time-course of pupal ovary development with (J) cartoons highlighting individual germaria from 12h APF, 30h APF and adults. Vasa (green) marks germline cells, Traffic Jam (TJ, white) marks somatic ICs, DAPI (blue) marks all nuclei, LaminC (red) marks Terminal Filament (TF) cells (cyan arrowheads in D-G) and Fas3 (also red) marks basal stalk cells, except in (A) where red signal is just from Hts staining. All scale bars, 20 μm. (A) At 0h APF ovaries are not yet organized into distinct germaria. The germline (green) consists of individual cells intermingled with somatic IC precursor cells (white). The medial side of the ovary, on the right, has more developed Terminal Filaments. "Apical cells", the precursors of epithelial sheath cells, are located at the apical (top) side of the ovary (white arrowhead). (B) At 12h APF ovaries are organized into distinct germaria, separated by a layer of migrating Apical cells. Lamin-C stains the nuclear envelope of Terminal Filament cells (cyan arrowhead). Fas3 staining is present on the medial side of the ovariole (pink arrowhead). TJ staining of somatic cells extends beyond the germline. (C) At 18h APF, basal stalks begin to form on the medial side of the ovary (pink arrowhead). (D) At 24h APF, Fas3 is spread more evenly around the circumference of the ovary, and stains a hub into which the posterior ends of the basal stalks converge.

(E) By 30h APF, individual germaria are farther apart, separated from one another by a layer of 1-2 epithelial sheath cells. Lamin-C staining appears in the transition cell at the posterior end of the terminal filament, and dimly in epithelial sheath cells. (F) At 36h APF, germaria are separated by 2-3 epithelial sheath cells. Lamin-C expression is increased in epithelial sheath cells, and is also now visible (red arrow) in Cap cells (CC). Basal stalks (pink arrowheads in E-G) begin to narrow. (G) By 48h APF, the basal stalks have narrowed, and Fas3 begins to be expressed dimly in posterior ICs (yellow arrowhead). Lamin-C expression in the Cap cells increases at this stage. White arrowhead points to Lamin-C expression in epithelial sheath cells. (H) At 56h APF, germaria begin to bud the first egg chamber. (I) At 102h APF, 3-4 egg chambers have budded. (J) Cartoons illustrating individual germaria at 12h APF, 30h APF and adult stages for comparison. In the adult Escort Cells (ECs) surround developing germline cysts (white), three layers of Follicle Stem Cells (FSCs) ring the germarial circumference immediately anterior (left) to a stage 2b germline cyst and strong Fas3 (red) staining on the surface of early Follicle Cells (FCs). Polar cells (cyan) are the source of the Upd ligand that activates JAK/STAT signaling, which stimulates FSC proliferation and conversion to FCs.

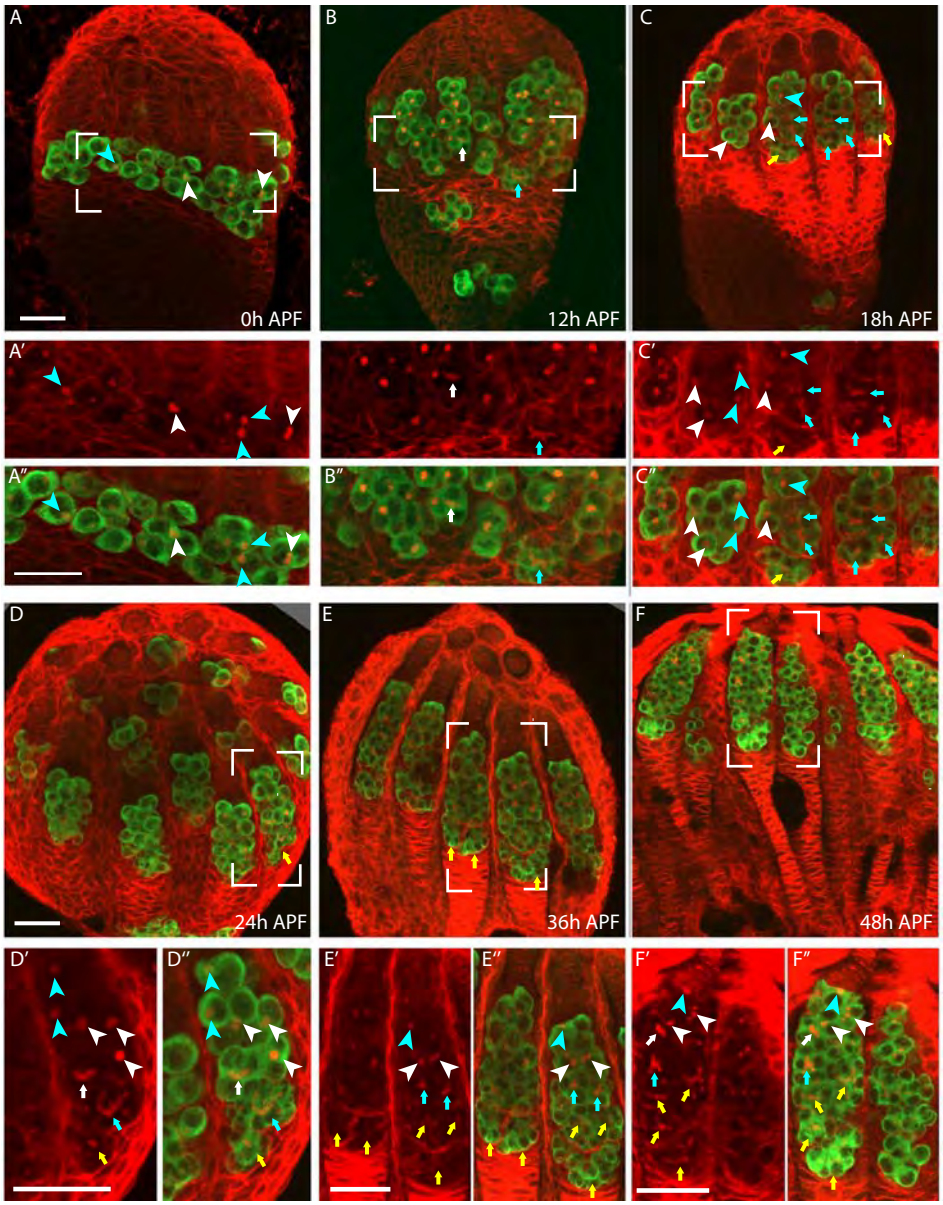

Figure 2. Germline development during early pupal stages.

(A-F) Germline development at the indicated times after puparium formation (APF) was monitored with Hts (red), which stains spherical spectrosomes and branched fusomes in germline cells as well as the surface of many somatic cells, and Vasa (green), which identifies germline cells. The number of germline cells within a cyst was determined by examining the fusome connecting clustered Vasa-positive cells over a range of z-sections (here, single or small numbers of superimposed z-sections are shown). For each sample, a close-up of the region outlined with white brackets is shown (A'-F') without or (A"-F") with the Vasa fluorescence channel. (A-F) Germaria progressively lengthen from anterior (apical, top, future anterior) to posterior (basal, bottom, future posterior) as germline cells become more numerous. The number of germline cells in a cyst is indicated as one (cyan arrowhead), two (white arrowhead), four (white arrow), eight (cyan arrow) or sixteen (yellow arrow). (B, D) Some germline cells migrate through the basal cells to become stranded at the posterior of the ovary. (A-A") At 0h APF germline cells are single cells (cyan arrowheads) or 2-cell cysts (white arrowheads). (B-B") At 12h APF the majority of germline cells have 1 or 2 cells, but posterior cysts may have 4 (white arrow) or 8 cells (cyan arrow). (C-C") At 18h APF, there is a large range of germarial length and corresponding posterior cyst maturity. Longer germaria have 16 cells in posterior cysts (yellow arrows) whereas short germaria have only 2 cells in posterior cysts (white arrowhead). (D-D") At 24h APF the majority of germaria have 16 cells in posterior cysts (yellow arrows) but the most posterior cyst has not yet moved beyond other cysts. (E-E") At 36h APF a single cyst resides at the posterior of most germaria but in some cases the most posterior 16-cell cyst has not yet been resolved. (F-F") By 48h APF each germarium has a most posterior 16-cell cyst. Scale bars, 20 micron.

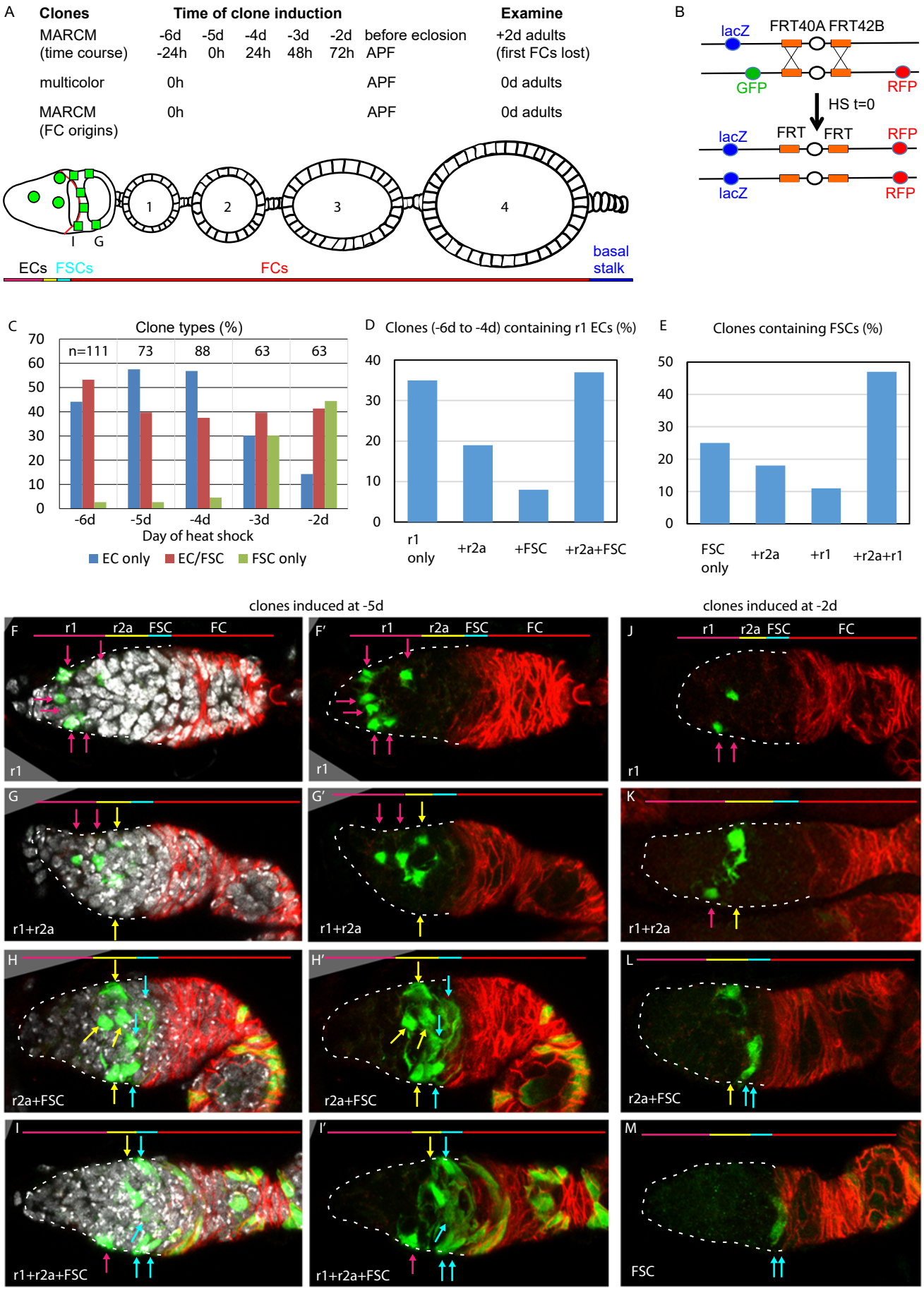

Figure 3. Common precursors for FSCs and ECs with derivatives clustered along the AP axis.

Figure 3. Common precursors for FSCs and ECs with derivatives clustered along the AP axis.

(A) Summary of lineage tracing experiments performed in this study. The ovariole of a newly eclosed adult, which has 4 egg chambers, is depicted with an example lineage (green cells). In the first set of experiments, we dissected ovarioles from adults 2d after eclosion ("+2d"), having induced clones daily (in separate experiments) between 6d and 2d before eclosion ("-6d" to "-2d"). In these experiments the first egg chambers to bud from the germarium will no longer be present and therefore the first FCs to be made cannot be seen. Some cells that had been FSCs at eclosion will have moved into the FC region posterior to the Fas3 border (red line). To capture all labeled FCs produced during pupation we examined newly-eclosed adults. To examine the maximal proportion of marked ovarioles with a lineage derived from a single cell we used multicolor labeling. (B) Second chromosome genotype of multicolor flies used for multicolor lineage tracing of precursors, showing tub-lacZ (lacZ), ubi-GFP (GFP) and His2Av-RFP (RFP) transgenes and FRT 40A and FRT 42B recombination targets either side of the centromere (white oval). Heat-shock induction of a hs-flp transgene on the X-chromosome can induce recombination independently at either pair of FRTs, making one or both chromosome arms homozygous in daughter cells, thereby eliminating one or more of the marker genes. A possible outcome for one daughter cell is shown. The other daughter has a complementary genotype (in this case with GFP-only), so that it is generally possible to identify sister "twin-spot" lineages. (A-K) GFP-labeled MARCM clones were induced from 6d to 2d before eclosion and flies were dissected 2d after eclosion. In each germarium labeled cells were scored as region 1 (r1) ECs, region 2a (r2a) ECs, or FSCs. (A) Most clones initiated 4-6d before eclosion contained only ECs (blue) or FSCs together with ECs (red), indicating a common precursor. Clones containing only ECs declined and clones containing FSCs but no ECs (green) increased in frequency when initiated at later times. (B, C) Data were pooled from clones induced from -4 to -6d. (B) Clones containing r1 ECs (n=174) were grouped according to the additional cell types they contained; inclusion of other r1 ECs was the most frequent, and r2a ECs were more commonly included than more distant FSCs even though the total frequency of clones with r2a ECs (54%) and FSCs (57%) were similar. (C) Clones containing FSCs (n=155) contained r2a ECs more frequently than r1 ECs even though the total frequency of clones with r2a ECs (54%) was lower than for r1 ECs (64%). (D-G) Examples of different clones induced 5d before eclosion all demonstrate the clustering of marked cells (green) along the anterior (left) to posterior (right) axis. The anterior Fas3 (red) border, viewed in each z-section, allows distinction between FCs and FSCs (in the three layers anterior to Fas3); several z-sections were combined to show all labeled cells in one image. DAPI (white) staining reveals all nuclei but is omitted in (D'-G') and (H-K) for clarity. GFP-marked clones have (D) a cluster of r1 ECs (magenta arrows), (E) a cluster of r1 and r2a ECs (yellow arrows), (F) a cluster of r2a ECs and FSCs (blue arrows), (G) r1 and 2a ECs with FSCs. (H-K) Clones induced 2d before eclosion also showed clustering of progeny, with (H) r1 ECs only, (I) r1 and r2a ECS, (J) r2a ECs and FSCs, and (K) FSCs only. Scale bars, 20 μm.

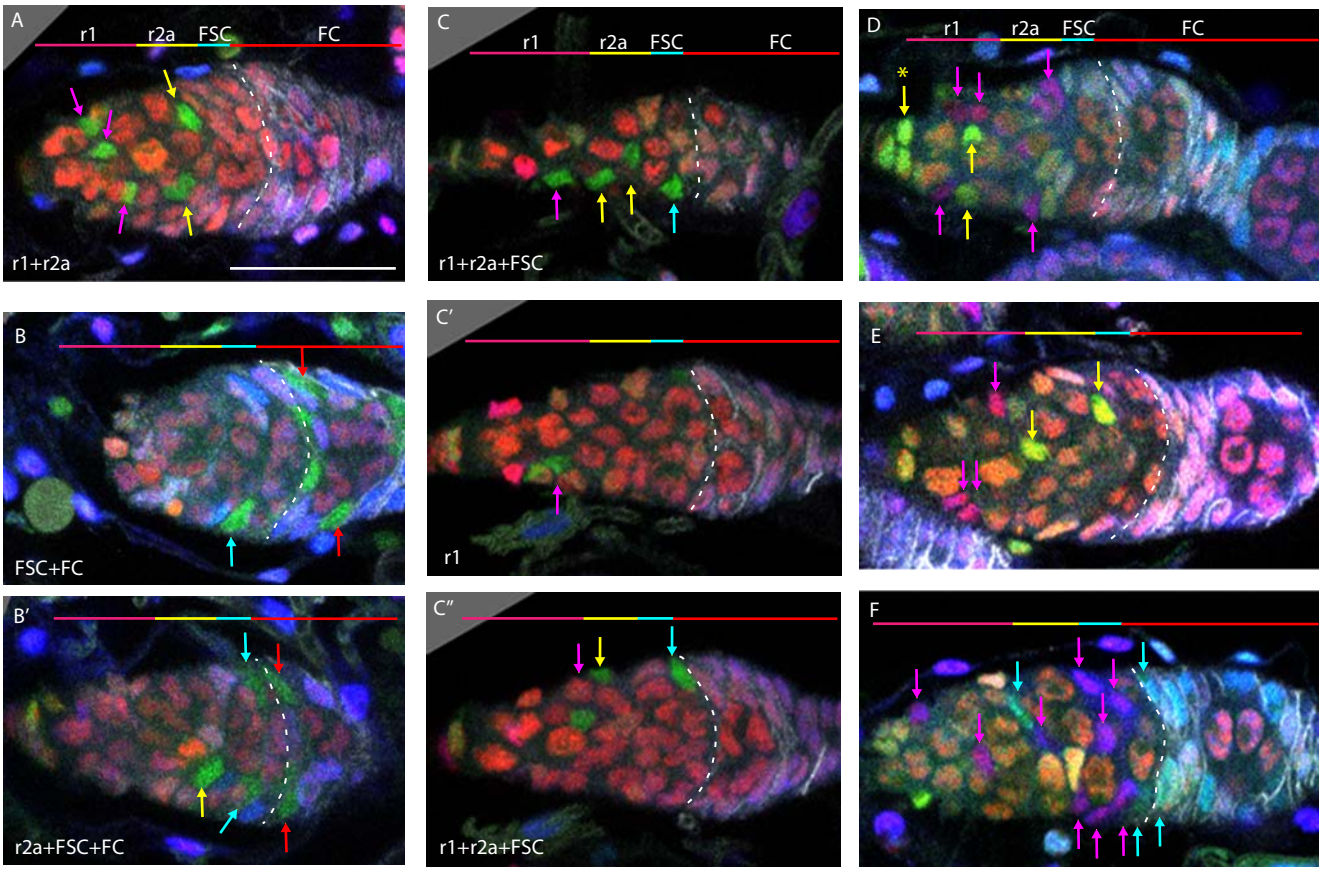

Figure 4. Multicolor labeling of precursors shows clustering of progeny along the AP axis.

(A-F) Multicolor lineage tracing was performed by inducing clones 5d before eclosion and dissecting newly-eclosed flies. The anterior limit of Fas3 staining is marked by a white dashed line. Scale bar in (A) applies to all images, 20 μm. Precursors produce r1 (magenta) and r2a (yellow) ECs, FSCs (cyan), and FCs (red) in overlapping zones, indicated by the colored zones and in (A-C) corresponding arrow colors. (A-C) show examples of GFP-only clones (green), which are generated by two recombination events and are therefore infrequent. (A) A clone containing r1 and r2a ECs. (B, B') Different z planes of a germarium show a clone containing an r2a EC, FSCs, and FCs. (C-C") Three z planes of a germarium showing a clone with r1 and r2a ECs and FSCs. (D-F) Examples of two clones of different colors in overlapping or adjacent zones, where arrow color indicates the clone color, not the cell type. (D) a GR (GFP plus RFP) clone (yellow arrows) contains r1 ECs and Cap cells (extreme left) and a BR (lacZ plus RFP) clone (magenta arrows) contains r1 and r2a ECs. (E) A BR clone (magenta arrows) contains r1 ECs and a GR clone (yellow arrows) contains a r2a EC and an FSC. (F) A BR clone (magenta arrows) contains ECs and FSCs, and a BG (lacZ GFP) clone (cyan arrows) contains a r2a EC, FSCs and FCs.

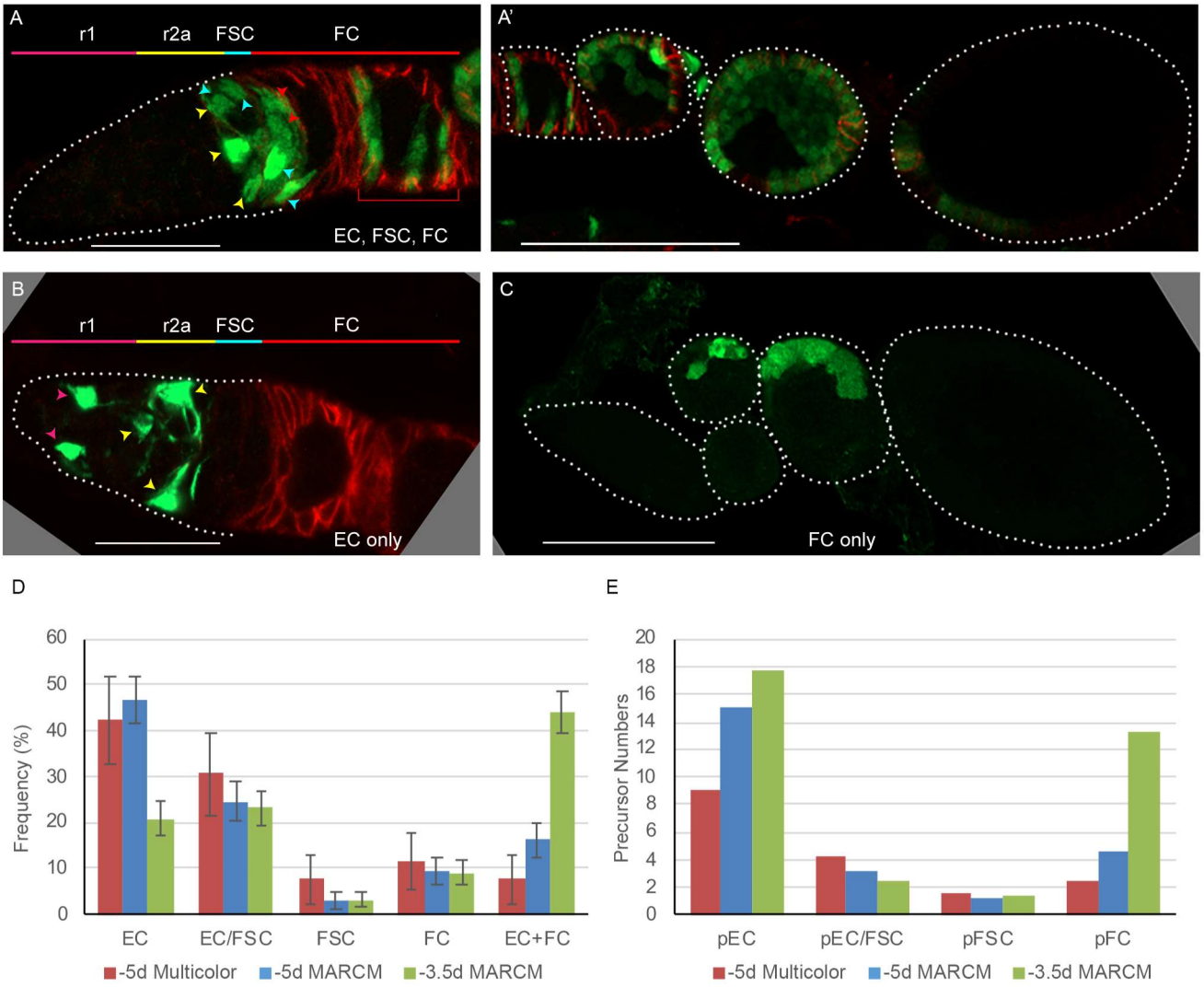

Figure 5. Follicle Cell origins and deduced precursor numbers for ECs, FSCs and FCs.

(A-C) GFP-labeled MARCM clones (green) were induced 5d before eclosion and ovaries were dissected from newly-eclosed adults in order to detect all FCs produced during pupation. Fas3 is stained in red and cell types are indicated with color-coded arrows, matching the labeled AP domains. Scale bar in (A, B), 20 µm; (A', C), 50 µm. (A) Germarium and (A') the rest of the ovariole of the same sample (the first egg chamber is in both images), showing a clone with marked ECs, FSCs and FCs (marked FCs are in the germarium and egg chambers 1-4). (B) A clone containing only ECs (no cells were marked in the rest of the ovariole). (C) A clone containing only FCs in egg chambers 2 and 3. (D) Distribution of clone types in GFP-only clones of multicolor flies and MARCM clones initiated 5d or 3.5d before eclosion, all examined in newly-eclosed adults. Clone types are: EC (EC-only), EC/FSC (ECs and FSCs, with or without FCs), FSC (with or without FCs), FC (FC-only), and EC + FC. Ovarioles with only marked ECs and FCs likely harbor two independent lineages. (E) Estimates of numbers of dividing precursor types at the time of clone induction for the same three lineage experiments as in (D), after accounting for double-clones (see Methods and Table 3). Precursor types are defined by their adult products: pEC (only ECs), pEC/FSC (ECs and FSCs, with or without FCs), pFSC (FSCs with or without FCs), and pFC (only FCs).

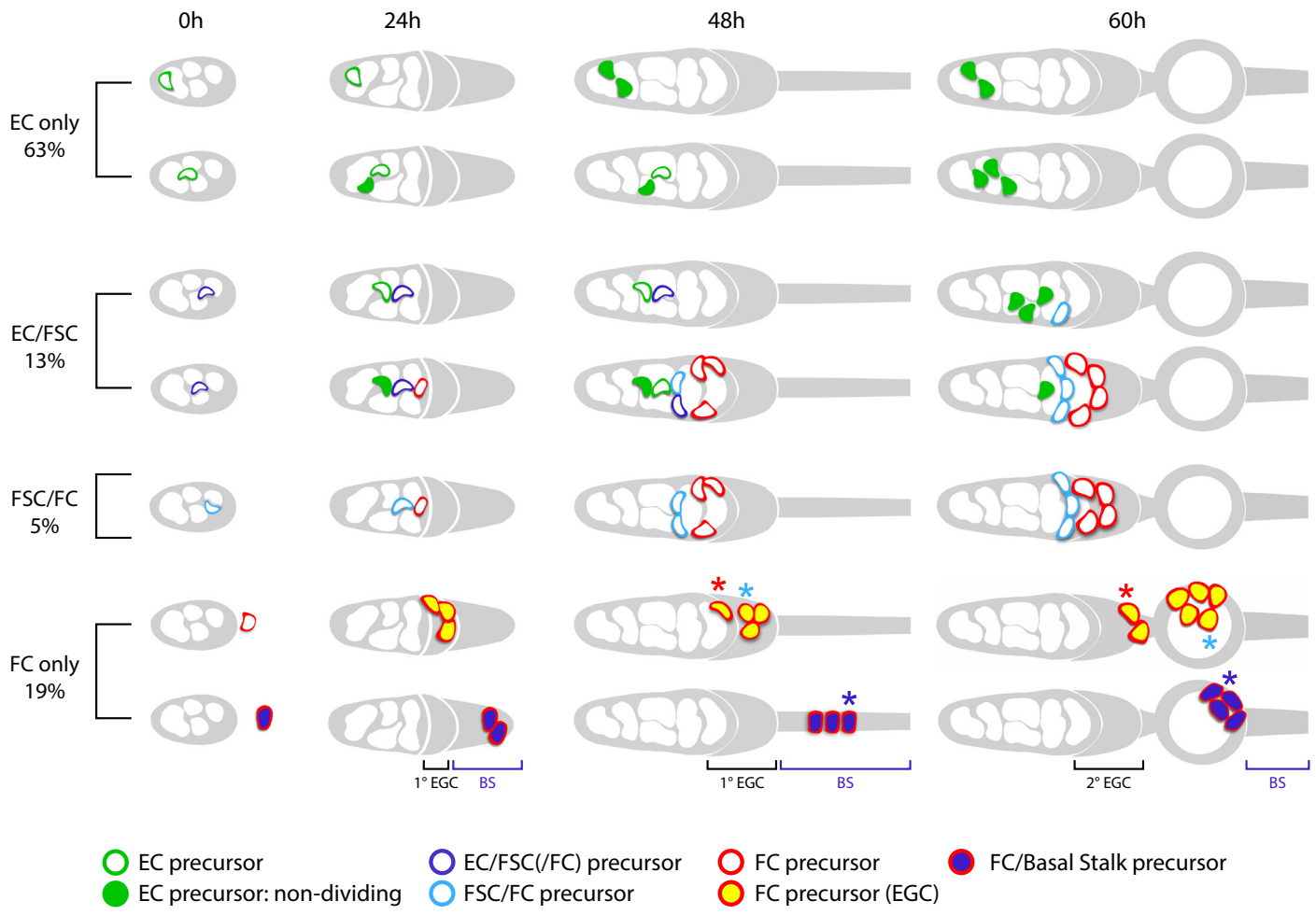

Figure 6. Summary of precursor lineage development

Cartoon of the fate of single precursor types from 0h APF until 60h APF deduced from lineage studies and pupal ovary imaging. The indicated frequency of clone types is drawn from the inference of single-cell lineages for MARCM clones induced at 0h APF (Table 3). Most 0h APF precursors (green) generate only adult ECs, with more anterior (left) precursors producing only r1 ECs (top row) and more posterior precursors also producing r2a ECs and more cells in total (second row). Filled green cells have ceased division. Most 0h APF FSC-producing precursors also produce ECs. Some of the more anterior precursors (third row) do not produce FCs but most (fourth row) produce cells that will become FCs (but not in the first-formed egg chamber). Precursors that produce adult FSCs but not ECs also produce FCs (fifth row). The most posterior precursors produce only FCs. Examples of origination from an EGC (row 6) and a basal stalk cells (row 7) are shown, but the most posterior ICs can also yield lineages containing only FCs. A subset of progeny accumulate posterior to the germarium from 24h APF onward in the EGC (depicted as the posterior gray crown). Most cells in the EGC will become FCs of the first budded egg chamber (sixth row). The cell on the posterior cyst at 48h APF, denoted by the red asterisk, moved into the secondary EGC at 60h and is modeled on the top red cell in Fig. 10. The cell denoted by the blue asterisk that is in the EGC at 48h APF and moved onto the first budded cyst at 60h is modeled after the cyan cell in Fig. 10. Most precursors present in the basal stalk at 48h APF (row 7) move onto the first budded cyst (the cell denoted by the blue asterisk is modeled after the white cell in Fig. 10). More posterior precursors are shown producing larger numbers of progeny because anterior cells divide more slowly and arrest division prior to eclosion.

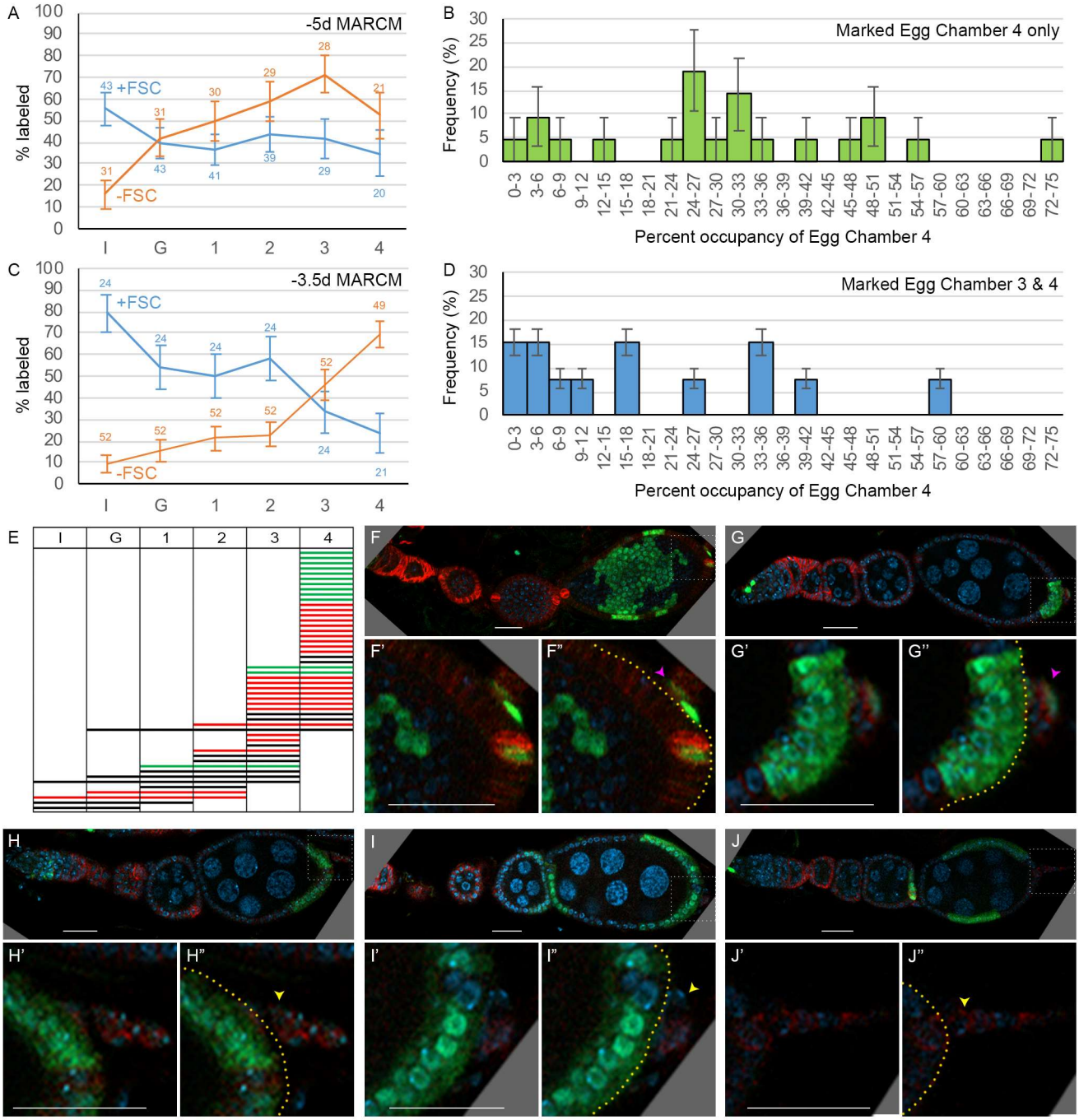

Figure 7. Patterns of FC contributions indicate distinct pools of precursors along the AP axis.

(A, C) Percentage of ovarioles containing labeled FCs that have marked FCs in germarial region 2b (I), region 3 (G), or egg chambers 1, 2, 3 or 4 (see Fig. 3A) in newly-eclosed adults for (A) -5d MARCM and (C) -3.5d MARCM clones with FSCs (blue line) or with no FSCs (orange line). The total number of ovarioles scored is indicated either side of the error bars (SEM); some ovarioles had only 3 egg chambers and some were not fully imaged. (B, D) MARCM clones induced at -3.5d and analyzed in newly-eclosed adults. Marked occupancy of egg chambers was scored as a percentage of all FCs in egg chamber 4 that were marked when there were marked FCs (B) only in Egg Chamber 4 or (D) in egg chambers 3 and 4. The frequency of different occupancy ranges is displayed in bins of 3%. (E) Distribution amongst germarial region 2b (I), region 3 (G) and egg chambers 1-4 of FC-only clones in newly-eclosed flies after marking at -3.5d. Each row indicates a single ovariole. The colors indicate if a marked cell is present in the basal stalk (green), absent from the basal stalk (red) or if the basal stalk was not clearly imaged (black). (F-J) Ovarioles of newly-eclosed flies with MARCM recombination induced at -3.5d containing FC-only clones. (F, G) Marked FCs can be seen in the basal stalk and egg chamber 4, (H) egg chamber 4 only, or (I, J) in egg chambers 4 and 3 only. Insets show enlargements of boxed regions; yellow borders outline the posterior edge of Egg Chamber 4, with cells further posterior located in the basal stalk. Yellow arrowheads (no marked basal stalk cell); Pink arrowheads (marked basal stalk cell). GFP: green; Fas3: red; DAPI: blue. Scale bars, 20 μm.

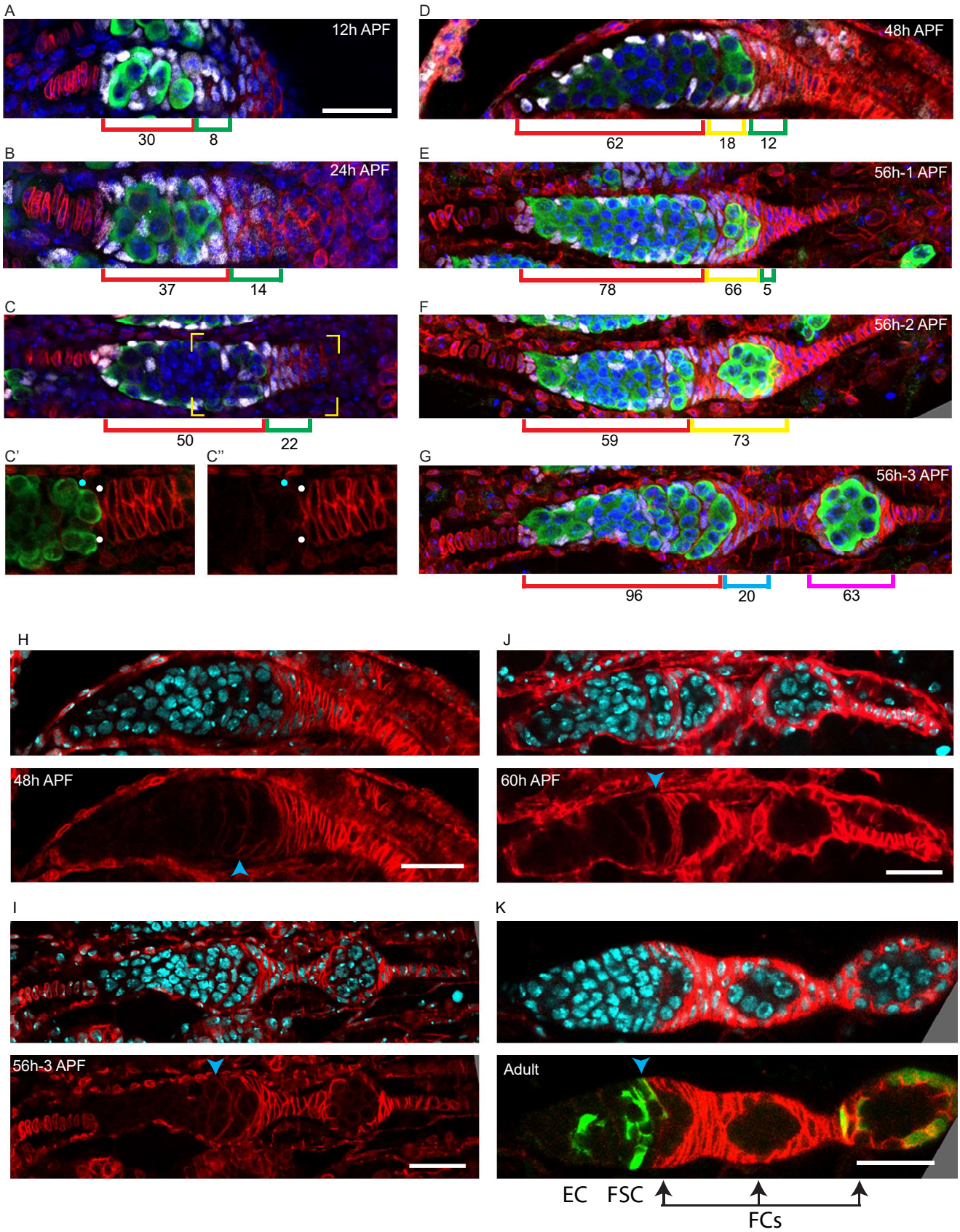

Figure 8. Extra-Germarial Crown Cells (EGCs); a potential source of early FCs.

Figure 8. Extra-Germarial Crown Cells (EGCs); a potential source of early FCs.

(A-G) Traffic Jam (TJ) positive cells (white) were counted in ovaries stained also for Vasa (green), LaminC and Fas3 (both in red), and DAPI (blue). Bar, 20 μm applies to all images. (A-C) Up to 36h APF, prior to budding of the first egg chamber, ICs (red brackets), defined as intermingled with germline cells (green) in the developing germarium, expressed TJ (white) but little or no detectable Fas3 (red). Cells posterior to the developing germaria expressed Fas3 and were previously all termed basal cells and expected to intercalate to form the basal stalk. However, a subset of Fas3-positive cells immediately posterior to the germarium also expressed TJ. Those cells formed an Extra-Germarial Crown (EGC) of increasing cell numbers, indicated by green brackets. (C', C") At 36h APF some somatic cells contacting the posterior of the most advanced cyst expressed Fas3 strongly (white dots) and some did not (blue dots). Fas3-positive cells were counted as EGC cells and Fas3-negative cells as ICs. (D) At 48h APF the most posterior germline cyst is about to leave the germarium in most samples. Here, the cyst (green) appears to have just started to leave, invading Fas3-positive cells in EGC territory. The Fas3-positive cells surrounding the cyst are indicated by a yellow bracket, while Fas3-positive and TJ-positive cells posterior to the cyst are indicated by green brackets. Average IC (red brackets) and EGC (green and yellow brackets) cell numbers are written underneath the brackets and were derived from counting (A) 5, (B) 5, (C) 10 and (D) 5 samples. (E-G) Three developing ovarioles from the same 56h APF ovary, representing progressively later stages of development from top to bottom, show the most posterior cyst leaving the germarium and surrounded by Fas3-positive, TJ-positive cells. (E, F) Fas3-positive, TJ-positive cells posterior to the germline (green bracket), and around the most posterior cyst (yellow bracket) were counted for these single samples and then (G) counted as on the budded cyst (magenta bracket) or anterior to the budded cyst and forming a secondary EGC posterior to the germarium (blue bracket). Those two populations are separated by stalk cells that do not stain for TJ. (H-K) Fas3 (red) is shown together with DAPI-stained nuclei (blue; top) or alone (bottom) in pupal ovaries at (H) 48h APF, (I) 56h APF (same samples as in (D) and (G)), (J) 60h APF and (K) adults. The anterior border of strong Fas3 expression (indicated by a blue arrowhead) was (C', C") posterior to all germline cysts at 36h APF, aligns (H) with the anterior of the departing cyst at 48h APF, (J, K) with the anterior surface of the most posterior germarial cyst just after one egg chamber has budded, and (J) by 60h APF and (K) in adults, the anterior edge of strong Fas3 expression is along the posterior edge of the penultimate cyst in the germarium. (K) Cells in a MARCM lineage (green) derived from an adult FSC (bottom panel) include an EC, FSCs and FCs (outlined by strong Fas3) in the budded egg chamber. Arrows indicate the normal progression every 12h of a recently produced strongly Fas3-positive FC associated with the penultimate germarial (stage 2b) cyst (first arrow) to an FC on a stage 3 germline cyst at the posterior of the germarium (second arrow) and then to an FC on a budded egg chamber (third arrow); 24h in total.

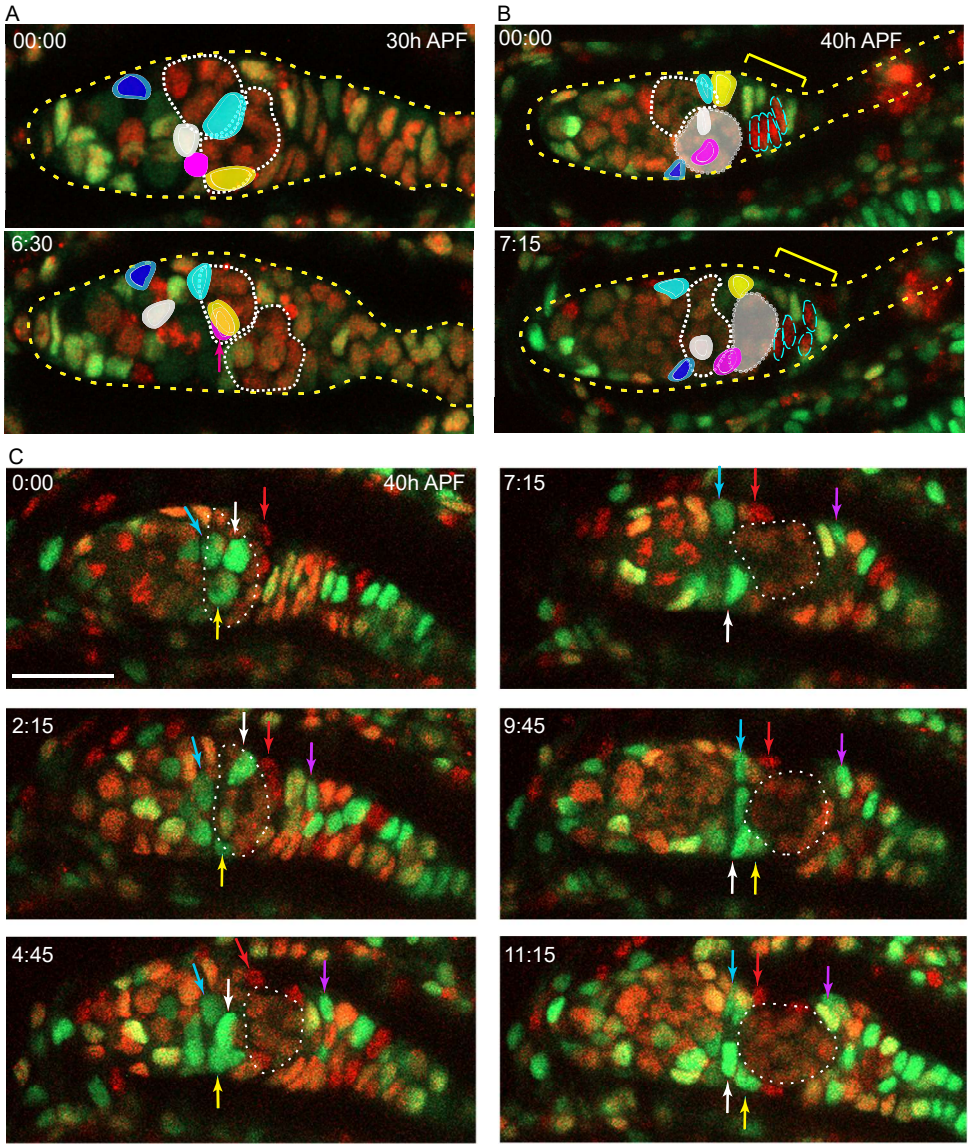

Figure 9. ICs move independently of one another and do not mix with EGCs.

Live imaging was performed on multicolor pupal ovaries with clones induced by heat shock such that cells could lose RFP, GFP, or both. (A) Z-projections of 0h and 6h30min timepoints of a 30h-APF germarium showing five tracked ICs (colored). ICs were located at the outer surface of the germarium and moved independently of one another in posterior, anterior, and lateral directions (around the circumference). The most posterior germline cyst (outlined by a white dotted line) moved posteriorly past the cyan and yellow IC cells. The relative disposition of ICs and cysts changed considerably, suggesting they are not strongly associated. Only z planes containing tracked cells were included in the projection (z4, 5, 6, 7, and 8 at 00:00 and z5, 6, 9, and 10 at 6:30) (B) Z-projections of 0h and 7h15min timepoints of a 40h-APF germarium showing five tracked ICs. ICs moved independently of one another and remained in their domain as the most posterior germline cyst (highlighted by shading) moved past. Four cells in the EGC (outlined red cells) remained in the EGC (indicated by the yellow bracket). Projected sections are z5-9 at 00:00 and z4, 7, 8 and 9 at 7:15. Individual z sections of the germaria in A and B are shown in Fig. S2. (C) Z-projections of selected timepoints of a 40h-APF germarium imaged for 11h15min, showing three tracked green ICs (white, yellow and blue arrows); ICs remained in their domain as the posterior germline cyst (outlined by a white dotted line) moved past them. Four red cells (one is shown by the red arrow) started on the posterior of the posterior cyst and moved anterior along the cyst; cells in a neighboring no-color clone moved similarly. A green cell that began in the EGC (magenta arrow) moved onto the posterior edge of the cyst. The accompanying Movie S1 of this germarium shows mitotic cells in the EGC and the stalk. Bar, 20 μm.

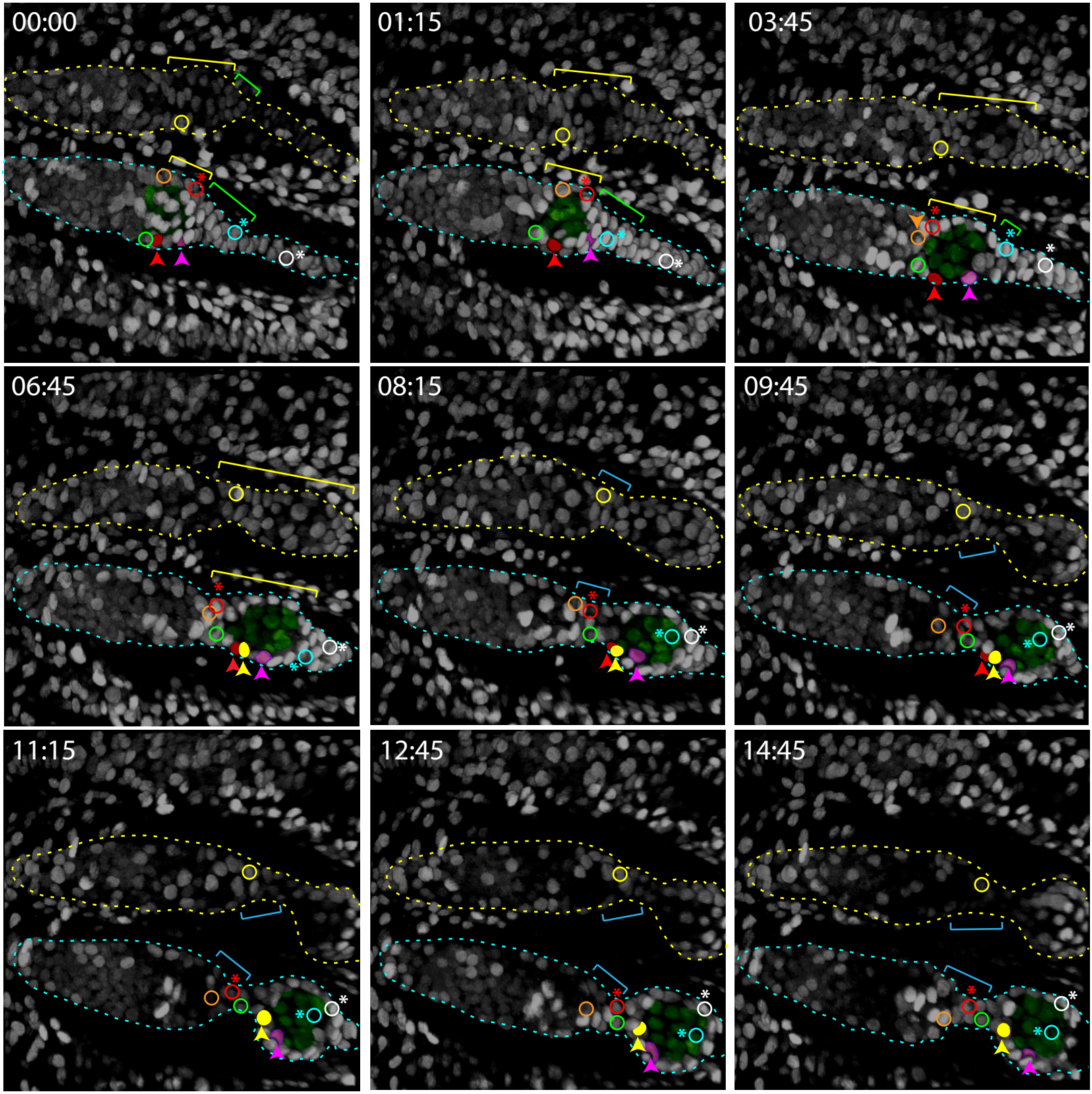

Figure 10. Budding of the first egg chamber: EGC cells become FCs.

Time-stamped frames from a 3D reconstruction of a movie of 14h 45 min starting at 48h APF and showing budding of an egg chamber. All cells are labeled white from a ubi-GFP transgene. Three cells that were visible near the surface of a 3D reconstruction are colored in solid red, pink, and yellow in the lower germarium, together with five other cells (open circles) that were in interior z slices. All marked cells were tracked using Zeiss Zen software for 60 time points over 14h 45 min, except for the red cell which could not be reliably tracked after 10h and the yellow cell in the lower germarium, which was not tracked before 5h 45min. The posterior germline cyst in the lower germarium is highlighted in green. Cyst cells were distinguishable from somatic cells because the nuclei were larger and paler green. The yellow brackets indicate Fas3+ TJ+ EGC cells, inferred from comparison to fixed images at the same stages.

The cyst slid past adjacent ICs, which were later either at the posterior edge of the germarium (orange-outlined cell and yellow-outlined cell in the upper germarium) or between the germarium and the budded cyst (green-outlined cell) in the nascent secondary EGC (magenta brackets), as seen more clearly in Fig. S2A, B (yellow-outlined cell) and Fig. S4A, B (orange and green-outlined cells). The cell marked with the open red circle (asterisk; modeled in Fig. 6) is inferred from comparison to fixed 48h APF images to be Fas3-positive and to be one of the most anterior EGC cells when the cyst first started to move out of the germarium (just prior to 48h APF, see Fig. 9). This cell began on the posterior cyst and ended in the secondary EGC (Movie S3). The cyan cell (asterisk; modeled in Fig. 6) initially towards the posterior of the primary EGC (indicated by yellow brackets) adopted progressively more anterior positions on the germline cyst after the cyst moved into EGC territory. The white cell (asterisk; modeled in Fig. 6) was originally in a location posterior to the EGC (it is expected, from comparison to fixed images, not to express TJ) but then moved into EGC territory by 3h 45min and ended up close to the cyan cell on the budded germline cyst (Movie S4). The locations of the cyan and white cells covering the posterior of the cyst can be seen clearly in Fig. S4. Individual z-sections showing the locations of the red, pink and yellow cells in the lower germarium at the beginning, middle, and end of their imaging times are shown in Fig.S3C and Movie S2. Time is in hours:minutes.

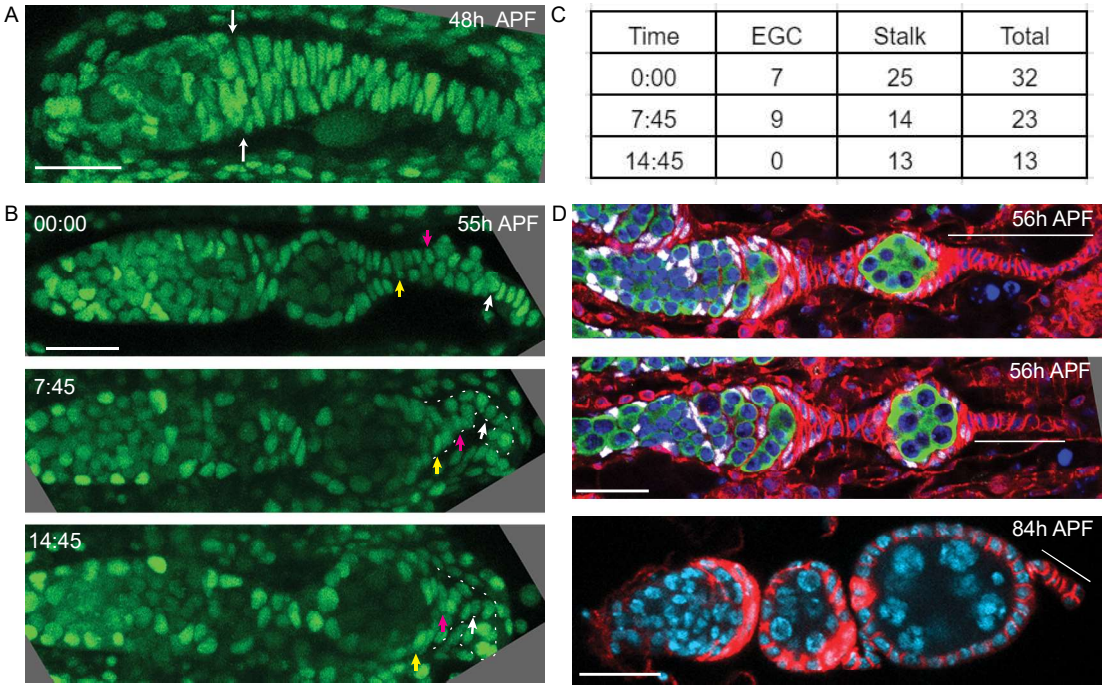

Time	EGC	Stalk	Total
0:00	7	25	32
7:45	9	14	23
14:45	0	13	13

Figure 11. Basal stalk and EGC cells are the source of the first FCs.

(A) Z-projection of a Ubi-GFP labeled germarium at 48h APF from live imaging to show the cells posterior to the germarium. White arrows indicate the posterior edge of the germline. (B) Stills from a movie of a 55h-APF germarium (Movie S6) show that the stalk, outlined by the white dotted line in the lower panels, progressively shortens as the first cyst moves posterior. Three cells were tracked: the white cell began in the stalk 13 cells away from the cyst and ended 4 cells away; the magenta cell was initially 7 cells away from the cyst and ended on the posterior of the cyst; and the yellow cell began as the first cell in the stalk and ended on the posterior third of the cyst. (C) Cell counts posterior to the germline for the germarium shown in (B). (D) Fixed images showing that the basal stalk becomes shorter over time. Thin white lines extend the length of the stalk. The top two images are stained for TJ (white), Vasa (green), DAPI (blue) and Fas3 (red). The lower image is stained for DAPI (blue) and Fas3 (red). After 2 egg chambers have budded there are an average of 9 cells in the stalk (n=12 stalks; the example in D has 9 cells). Scale bars, 20 μm.

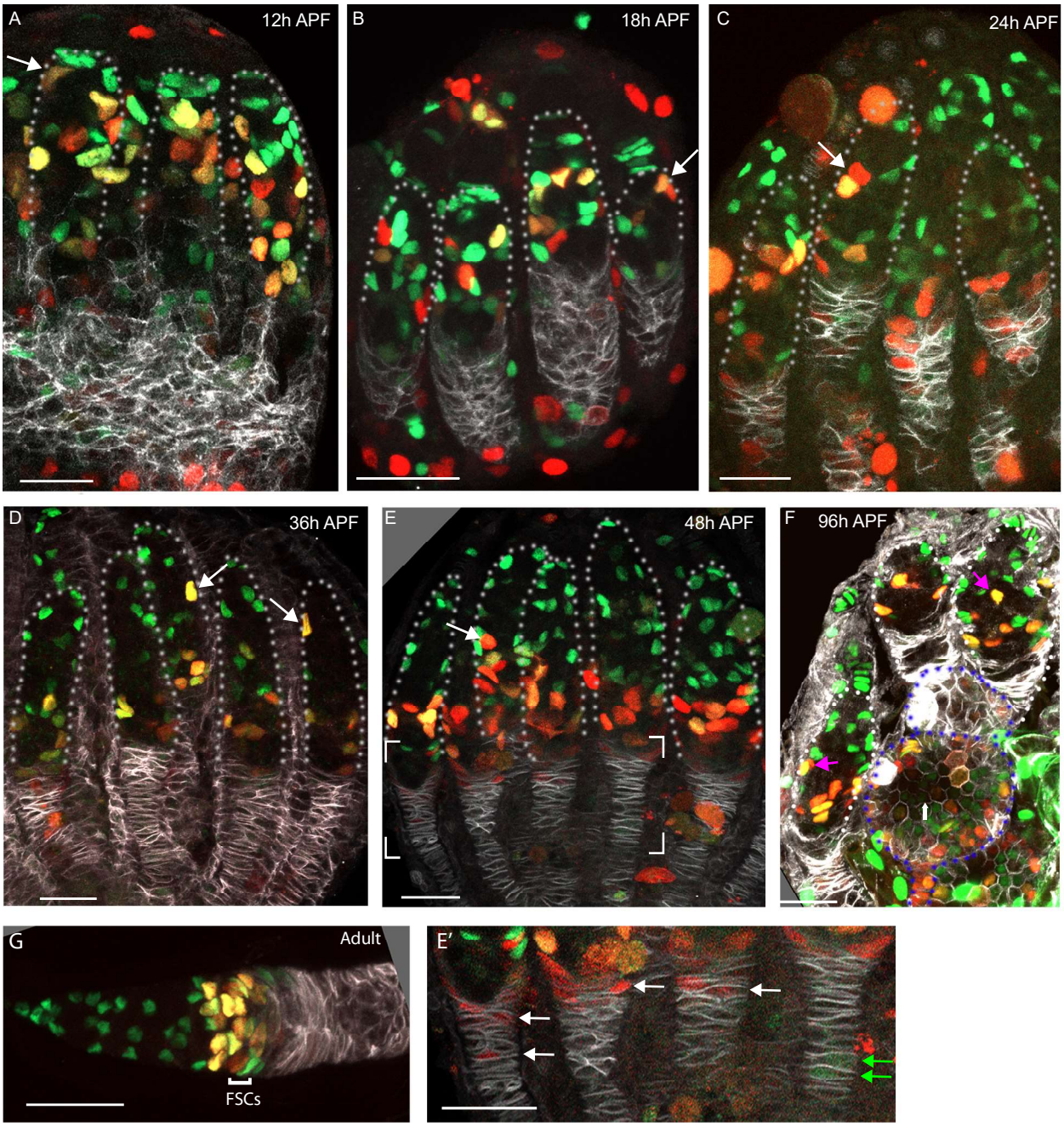

Figure 12. FUCCI labeling shows progressive accumulation of anterior ICs in G1 or a G0 arrest.

(A-G) C587-GAL4 was used to drive UAS-FUCCI expression and ovaries were stained for Fas3 (white) and TJ (not shown) to identify all somatic cells. Somatic cells were either green (G1 or G0), red (late S phase), red/green (G2) or without any color (early S-phase for cells with adequate C587-GAL4 expression). Germaria are outlined with dotted lines. All bars, 20 μm. (A-F) Many red or red/green cells are present in anterior locations close to Cap Cells at (A)12h APF and (B)18h APF (arrows) but (C) by 24h APF and (D) 36h APF fewer such cells are evident and are further from the anterior (arrows). (E) At 48h APF ICs in the anterior third of the germarium are uniformly green (G1 or G0). The bracketed region is magnified with enhanced colors to reveal (E') that many cells in the EGC are red (S-phase), while one or two more posterior, basal stalk cells are faintly green but C587-GAL4 expression is low at these locations. (F) At 96h APF, after three egg chambers have budded (two are outlined with blue dotted lines), red/green ICs can still occasionally be seen in the anterior half of the germarium (pink arrows) but (G) in adults this territory, occupied by r1 ECs, is entirely green, followed by a mix of green and red/green more posterior r2a ECs, and FSCs, which are predominantly red/green (G2), red or colorless (S-phase) and with only a few green (G1) cells. In adults, C587-GAL4 expression extends through all ECs and FSCs but ends near the FSC/FC border.

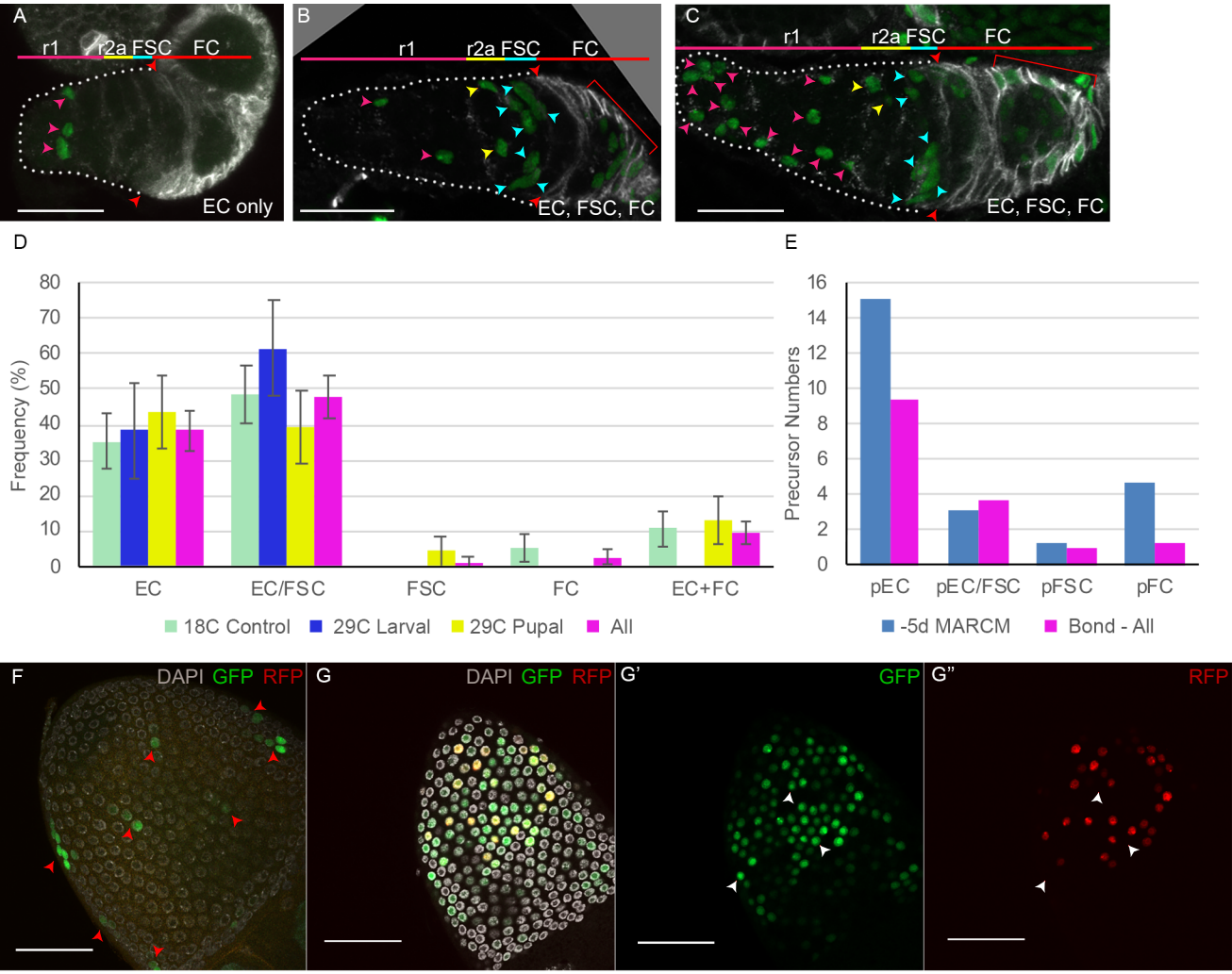

Figure 13. Lineages induced by bond-GAL4 reveal typical IC precursor patterns and a later EGC contribution. (A-G) bond-GAL4/G-TRACE clones (green) were examined in 0-12h adult ovaries, stained with antibodies to Fas3 (white in (A-C)) and DAPI (white in (F, G)). (A-C) For animals maintained at 18C throughout development, we observed mainly (A) marked ECs only or (B, C) marked ECs, FSCs and FCs; scale bars, 20 µm. (D) Distribution of clone types observed for animals kept at 18C throughout (green), raised at 29C and moved to 18C 2d after pupariation ("29C larval", blue), raised at 18C and moved to 29C for the last 3-4d of pupation ("29C pupal", yellow), or the aggregate of all results (pink). EC/FSC and FSC categories almost always included FCs also. (E) Estimates of precursor numbers for MARCM clones induced 5d before eclosion (blue) and for the aggregate of all bond-Gal4 lineages (pink) after disaggregating raw data into single lineages (see Methods). (F) Posterior egg chamber (29C larval) with small GFP clones (arrowheads). Multiple z-sections are projected to show all clones. (G) Posterior egg chamber (29C pupal) with patches of (G') GFP-positive cells, some of which also express (G") RFP, indicating relatively recent expression of bond-GAL4. (F-G) Scale bars, 50 µm.